COGNITIVE NEUROSCIENCE

Postnatal immune activation causes social deficits in a mouse model of tuberous sclerosis: Role of microglia and clinical implications

Manuel F. López-Aranda[1], Ishanu Chattopadhyay[2,3], Gayle M. Boxx[4], Elizabeth R. Fraley[5], Tawnie K. Silva[1], Miou Zhou[1], Miranda Phan[1], Isaiah Herrera[1], Sunrae Taloma[1], Rochelle Mandanas[1], Karen Bach[1], Michael Gandal[6], Daniel H. Geschwind[6], Genhong Cheng[4], Andrey Rzhetsky[2,3,7], Stephanie A. White[5], Alcino J. Silva[1]*

There is growing evidence that prenatal immune activation contributes to neuropsychiatric disorders. Here, we show that early postnatal immune activation resulted in profound impairments in social behavior, including in social memory in adult male mice heterozygous for a gene responsible for tuberous sclerosis complex (*Tsc2*$^{+/-}$), a genetic disorder with high prevalence of autism. Early postnatal immune activation did not affect either wild-type or female *Tsc2*$^{+/-}$ mice. We demonstrate that these memory deficits are caused by abnormal mammalian target of rapamycin–dependent interferon signaling and impairments in microglia function. By mining the medical records of more than 3 million children followed from birth, we show that the prevalence of hospitalizations due to infections in males (but not in females) is associated with future development of autism spectrum disorders (ASD). Together, our results suggest the importance of synergistic interactions between strong early postnatal immune activation and mutations associated with ASD.

INTRODUCTION

There is growing evidence that prenatal viral infections constitute a risk factor for neuropsychiatric disorders, including schizophrenia and autism spectrum disorders (ASD) (*1*). Tuberous sclerosis (TSC) is an autosomal dominant disorder caused by mutations in either the TSC1 (9q34) or TSC2 (16p13.3) genes (*2*, *3*). TSC is the second most common neurocutaneous disorder, affecting 1 in 6000 people worldwide. Most patients with TSC are affected by a neuropsychiatric disorder (*4*), including ASD, which affects 40 to 61% of these patients (*5*, *6*).

Although previous results (*7*–*17*) showed that infections during early prenatal development can increase the incidence of specific neuropsychiatric phenotypes, little is known about the impact of infections late (i.e., postnatally) during development (*18*–*20*). Here, we reveal the molecular and cellular mechanisms of social memory deficits in mice mutant for the Tsc2 gene with postnatal immune activation. Our human studies also attest to the importance of immune activation (strong enough to require hospitalization) late in development in ASD.

[1]Departments of Neurobiology, Psychology, and Psychiatry, Integrative Center for Learning and Memory, and Brain Research Institute, University of California, Los Angeles, Los Angeles, CA, USA. [2]Department of Medicine and Human Genetics, Section of Computational Biomedicine and Biomedical Data Science, and Institute for Genomics and Systems Biology, University of Chicago, Chicago, IL, USA. [3]Department of Medicine, University of Chicago, Chicago, IL, USA. [4]Department of Microbiology, Immunology, and Molecular Genetics, University of California, Los Angeles, Los Angeles, CA, USA. [5]Department of Integrative Biology and Physiology, University of California, Los Angeles, Los Angeles, CA, USA. [6]Department of Neurology, Center for Autism Research and Treatment, Semel Institute, David Geffen School of Medicine, University of California, Los Angeles, Los Angeles, CA, USA. [7]Department of Human Genetics, University of Chicago, Chicago, IL, USA.
*Corresponding author. Email: alcinojsilva@gmail.com

RESULTS

Early postnatal immune activation induces long-lasting social memory deficits in adult *Tsc2*$^{+/-}$ male mice

Male and female *Tsc2*$^{+/-}$ mice and their wild-type (WT) littermates (WT mice) were injected with either polyinosinic:polycytidylic acid (Poly I:C; 20 mg/kg) or saline (control) intraperitoneally at postnatal day 3 (P3), P7, and P14 (Fig. 1A). We then tested the mice as adults (4 to 6 months old) in the three-chamber social interaction test (SIT) (*21*). Although all groups showed normal social interaction (Fig. 1B and fig. S1B), only male (but not female; fig. S1C) *Tsc2*$^{+/-}$ mice injected with Poly I:C early postnatally (*Tsc2*$^{+/-}$ Ep) showed social memory deficits (no preference for the novel mouse versus the familiar mouse in the social memory test; Fig. 1C). This social memory deficit was independently confirmed by two scientists in A.J.S.'s laboratory (fig. S2, A and B), as well as with an alternative protocol for social memory test (fig. S2, C and D) (*22*), demonstrating the robustness of this phenotype. All groups tested (fig. S3A) showed equivalent performance in the object recognition memory task (fig. S3B) (*23*), indicating that their social memory deficit is not due to deficits in memory for objects ("object memory"). In addition, unlike early postnatal injections, adult Poly I:C injections do not trigger chronic deficits in social memory in *Tsc2*$^{+/-}$ male mice (fig. S4, A and B). Together, these data indicate that in the first 2 weeks of life, *Tsc2*$^{+/-}$ male mice are especially sensitive to immune activation.

Transcriptomic alterations point to microglial activation and an elevated interferon response

To explore the mechanisms of social memory phenotypes described above, we performed RNA sequencing (RNA-seq) studies in three brain regions (prefrontal cortex, hippocampus, and cerebellum) previously implicated in social phenotypes (*24*–*26*). Previous studies have implicated the cerebellum (*26*–*29*) and prefrontal cortex

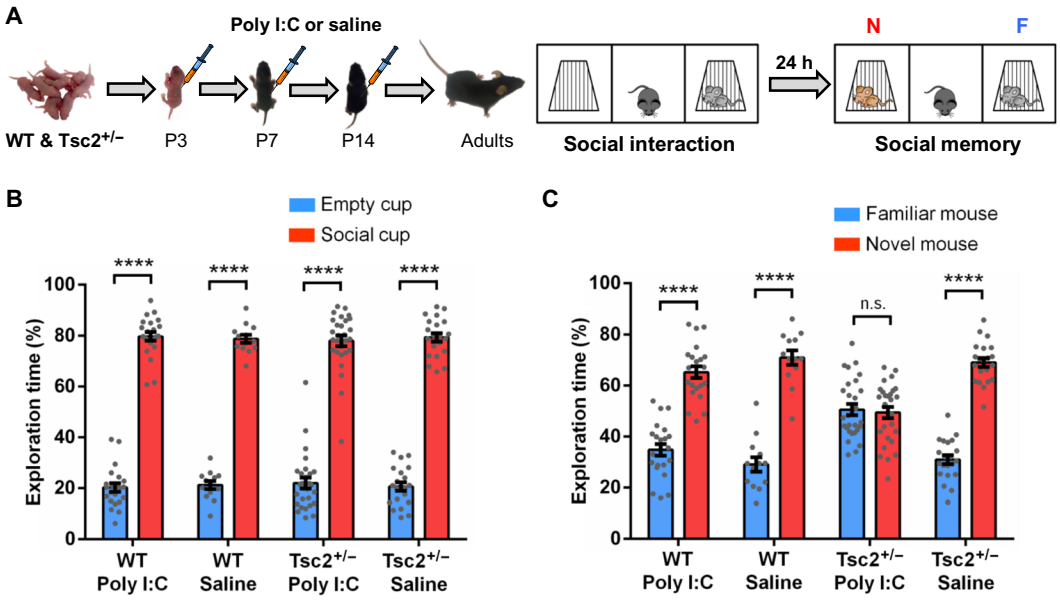

Fig. 1. Early postnatal immune activation triggers social memory deficits in adult *Tsc2*$^{+/-}$ male mice. (**A**) Timeline of injections of Poly I:C or saline and behavior approach. N, novel mouse; F, familiar mouse. (**B**) Graph shows the % of time that male mice spent actively exploring the empty and the social cups. WT/Poly I:C ($n = 22$; $P < 0.0001$, $t = 24.72$), WT/saline ($n = 13$; $P < 0.0001$, $t = 25.74$), *Tsc2*$^{+/-}$/Poly I:C ($n = 28$; $P < 0.0001$, $t = 18.75$), and *Tsc2*$^{+/-}$/saline mice ($n = 21$; $P < 0.0001$, $t = 24.90$) show normal social interaction (they explore significantly more the social cup than the empty cup). Analyses of the data using two-way analysis of variance (ANOVA) revealed no significant differences between groups. (**C**) Graph shows the % of time that male mice spent actively exploring the cups with the familiar mouse and the novel mouse. WT/Poly I:C ($n = 22$; $P < 0.0001$, $t = 9.43$), WT/saline ($n = 13$; $P < 0.0001$, $t = 10.35$), and *Tsc2*$^{+/-}$/saline mice ($n = 13$; $P < 0.0001$, $t = 15.34$) show normal social memory (they explore significantly more the novel mouse than the familiar mouse), but *Tsc2*$^{+/-}$/Poly I:C ($n = 28$; $P = 0.715$, $t = 0.36$) mice show social memory deficits (show no preference for the novel mouse). Two-way ANOVA analyses using time spent exploring the novel mouse as the dependent variable revealed a significant treatment × genotype interaction [$F(1,80) = 8.68$, $P = 0.0042$], and Sidak post hoc test revealed a simple main effect of genotype on the Poly I:C group ($P < 0.0001$, $t = 5.33$). Data represent means ± SEM as well as values for individual mice.

(*24*, *30*–*32*) in social phenotypes, including social interaction and social memory. Moreover, previous papers have also implicated those areas in social communication calls (*26*, *33*–*35*). Across regions, we identified 17 genes exhibiting differential expression [false discovery rate (FDR) < 0.1] (fig. S5) ~4 months after Poly I:C exposure (Fig. 2A) in *Tsc2*$^{+/-}$ Ep male mice compared with controls. As a class, known markers of microglia were significantly enriched among up-regulated genes (table S1), suggesting activation of this cellular population (FDR < 0.0002) (Fig. 2B). The RNA-seq results reported could reflect changes in cells other than microglia (e.g., macrophages). However, multiple convergent lines of evidence presented here demonstrate that changes in microglia are a key contributor to the social memory deficits of the Tsc2 mice with early postnatal immune activation. Further, we also observed significant enrichment of interferon (IFN) response genes among the up-regulated differential expression signal (FDR < 0.06) (Fig. 2B). These results mirror previous findings in ASD (Fig. 2C) (*36*) and point to a lasting up-regulation of microglia and IFN response pathways, which may underlie behavioral changes in *Tsc2*$^{+/-}$ Ep male mice. The analyses reported here represent the main effects all across three brain regions, which were done to identify regionally consistent, robust effects. Some of the top affected genes show complete or near-complete separation in expression between groups, representing large-effect changes. When analyzed within each brain region individually, we identified 137 differentially expressed genes at FDR < 0.1 or 104 genes at FDR < 0.05. Data file S1 includes a full summary statistic for all differential expression results.

Adult depletion of microglia results in the permanent rescue of the social memory deficits of male *Tsc2*$^{+/-}$ Ep mice

The results described above suggest that early postnatal immune activation increased IFN production by adult microglia in *Tsc2*$^{+/-}$ Ep male mice, thus leading to social memory deficits. Inhibition of the colony-stimulating factor 1 receptor (CSF1R) results in the elimination of ~99% of all microglia brain-wide (Fig. 3B) (*37*), and therefore, we treated *Tsc2*$^{+/-}$ Ep male mice with a CSF1R inhibitor (PLX5622 chow or vehicle control chow; Fig. 3A) for 21 days and then tested social memory. Treatment with PLX5622 completely rescued the social memory deficits of *Tsc2*$^{+/-}$ Ep male mice (Fig. 3C), and the rescue is still present when microglia repopulate the brain 2 months later (Fig. 3D).

Unlike *Tsc2*$^{+/-}$ Ep males, *Tsc2*$^{+/-}$ Ep female mice do not show social memory deficits (fig. S1C), a result that could be due to differences in microglia development (*38*). To test whether adult repopulation of microglia may reopen a window of sensitivity to immune activation in adult male and female *Tsc2*$^{+/-}$ mice, we first depleted the microglia of adult *Tsc2*$^{+/-}$ male and female mice with a 21-day PLX5622 treatment. During the repopulation and maturation of the new microglia population, we injected the mice with Poly I:C (20 mg/kg; Fig. 4A) and then tested social memory 6.5 weeks after the last Poly I:C injection. Although this treatment did not affect social interaction [discrimination index (DI) for social cup in male: 79.73%, $P < 0.0001$; DI in female: 69.76%, $P < 0.001$], it disrupted social memory in *Tsc2*$^{+/-}$ male and female mice (Fig. 4, B and C). Nevertheless, subsequent microglia depletion was able to rescue

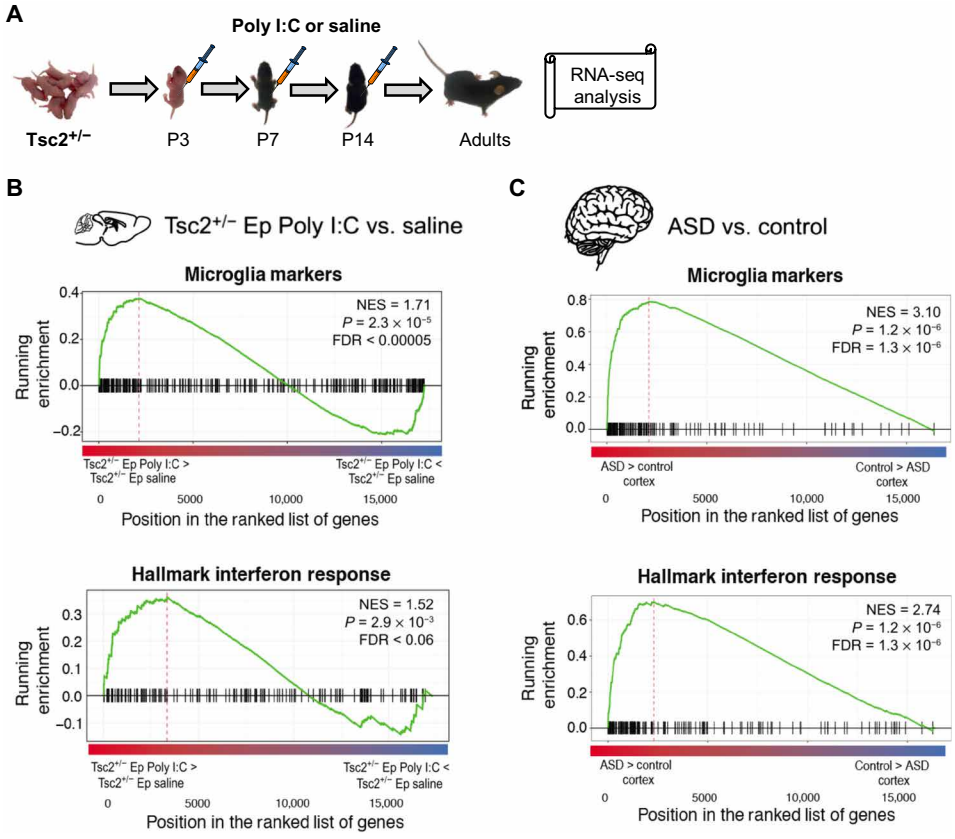

Fig. 2. Gene expression changes in the brain of *Tsc2*$^{+/-}$ mice with early postnatal immune activation. (**A**) Timeline for injections of Poly I:C. (**B**) Up-regulated genes are enriched for microglial markers and IFN response pathways, as shown by gene set enrichment analyses. Genes are ranked by differential expression $\log_2$ fold change. NES, normalized enrichment statistic. (**C**) Analogous enrichment of microglia and IFN response pathways is observed among up-regulated genes in ASD from postmortem frontal and temporal cortex samples compared with matched controls.

this social memory phenotype in both males and females (fig. S6, B and C). These results strongly support the hypothesis that immune activation during a sensitive period of microglia developmental can lead to permanent social memory deficits in *Tsc2*$^{+/-}$ mice.

Postnatal immune activation causes permanent social memory deficits in mice with the *Tsc2*$^{+/-}$ mutation restricted to microglia

To directly test the critical role of microglia in the social memory deficits of *Tsc2*$^{+/-}$ mice, we restricted this mutation to microglia (*39*). Specifically, we tested whether the injection of Poly I:C during microglia repopulation in adult male and female mice could trigger social memory deficits in a Cx3cr1^{Cre}-Tsc2^{Flox} mouse model with a floxed Tsc2 allele specifically deleted in microglia by Cre recombinase expressed from a microglia-specific promoter (Cx3cr1) (*39*). Although a previous study with Cx3cr1-Cre; Tsc1 mutant mice (*40*) reported spontaneous seizures, in the Cx3cr1-Cre; Tsc2 mice that we tested, we have never observed evidence for seizures.

After a 21-day PLX5622 treatment, we injected mice with Poly I:C (20 mg/kg) during microglia repopulation (Fig. 5A) and then tested social memory as described above. All groups showed normal social interaction (fig. S7C), but Cx3cr1^{Cre}-Tsc2^{Flox} male and female mice with the immune activation treatment showed robust social memory deficits (Fig. 5C).

We also repeated the studies just described with mice with a tamoxifen-inducible *Tsc2*$^{+/-}$ mutation restricted to microglia (the Cx3cr1^{CreER}-Tsc2^{Flox} mouse model) (*41*) that could be specifically triggered in adults. Because the induction of the Tsc2 deletion in the Cx3cr1^{CreER} mice precluded early postnatal immune activation, as carried out for the *Tsc2*$^{+/-}$ mice, in the Cx3cr1^{CreER}-Tsc2^{Flox} mice, we tested the role of immune activation in social memory after microglia repopulation in adult mice. We confirmed that 4-hydroxytamoxifen (4-OHT) did not affect social interaction (DI for social cup in male: 75.49%, $P < 0.001$; DI in female: 75.91%, $P < 0.001$) or social memory (DI for novel mouse in male: 59.52%, $P < 0.05$; DI in female: 59.2%, $P < 0.001$) in the Cx3cr1^{CreER}-Tsc2^{Flox} mice. Although all groups showed normal social interaction (fig. S7D), Cx3cr1^{CreER}-Tsc2^{Flox} mice (male and female) injected with 4-OHT (for Cre recombinase activation), and later injected with Poly I:C after PLX5622 treatment, showed a robust social memory deficit (Fig. 5D). These results demonstrate that activation of the *Tsc2*$^{+/-}$ mutation specifically in microglia in adults together with immune activation is sufficient to cause social memory deficits in *Tsc2*$^{+/-}$ mice.

The IFN-alpha/beta receptor α chain knockout prevents social memory deficits induced by early postnatal immune activation in *Tsc2*$^{+/-}$ Ep male mice

Prompted by our RNA-seq results, we evaluated the role of type I IFN signaling on the social memory phenotype of male *Tsc2*$^{+/-}$ Ep mice. Although male *Tsc2*$^{+/-}$ Ep mice showed robust social memory deficits (Fig. 1C), male *Tsc2*$^{+/-}$ Ep mice with a null mutation for the

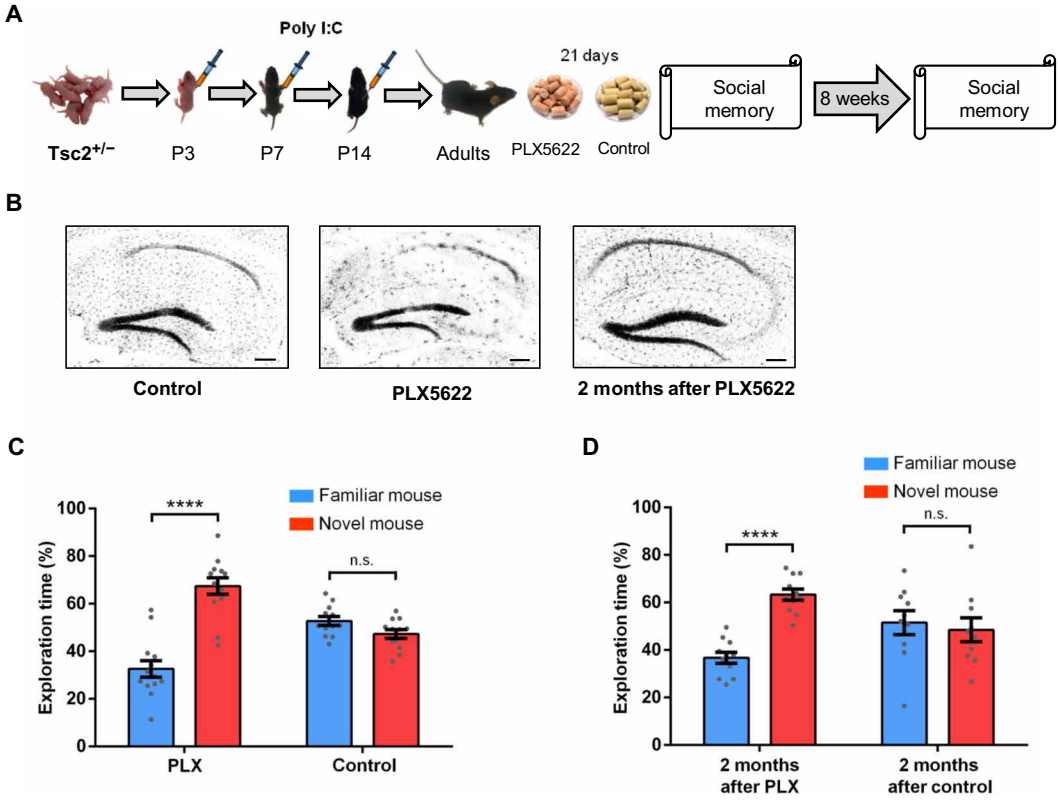

Fig. 3. Effects of microglia depletion in male *Tsc2*$^{+/-}$ Ep mice. (**A**) Timeline for injections of Poly I:C, treatment with PLX5622 (PLX; depletes microglia) or control chow and behavior approach. (**B**) IBA1 immunostaining of *Tsc2*$^{+/-}$ control, PLX, and 2 months after PLX mice. The treatment with PLX led to the elimination of most microglia in the whole brain (hippocampus shown as example) compared to the control group (hippocampus shown as example). Two months after PLX, the microglia had repopulated the brain (hippocampus shown as example). (**C**) *Tsc2*$^{+/-}$/PLX mice ($n = 13$; $P < 0.0001$, $t = 7.10$), but not *Tsc2*$^{+/-}$/control ($n = 12$; $P = 0.0502$, $t = 2.07$) mice, show normal social memory. (**D**) *Tsc2*$^{+/-}$ mice 2 months after PLX ($n = 11$; $P < 0.0001$, $t = 8.11$), but not *Tsc2*$^{+/-}$ mice 2 months after control ($n = 10$; $P = 0.67$, $t = 0.42$), show normal social memory. Data represent means ± SEM as well as values for individual mice. Scale bars, 200 μm.

IFN-alpha/beta receptor alpha chain gene (*Tsc2*$^{+/-}$/IFNAR1$^{-/-}$ Ep mice) showed normal social memory (Fig. 6, A and B). These results demonstrate the role of type I IFN signaling in the social memory deficits of *Tsc2*$^{+/-}$ Ep mice. Although we could have used other methods to address this possibility, including antibodies specific to IFNβ, we used a genetic approach because of its specificity and ease of use.

Two hours after a Poly I:C injection (*42*, *43*), *Tsc2*$^{+/-}$ mice showed a significantly higher level of IFNβ (type I IFN) compared to their WT littermates (Fig. 7, A and C), and this could be reversed by rapamycin [5 mg/kg; mammalian target of rapamycin (mTOR) inhibitor (*44*)] given at the same time as Poly I:C (Fig. 7, B and D). Rapamycin (5 mg/kg) also can prevent (Fig. 8, A and C) and permanently rescue (Fig. 8, B and D) the social memory deficits of *Tsc2*$^{+/-}$ Ep male mice, a result with considerable implications for the treatment of social phenotypes in TSC patients with ASD.

Early postnatal immune activation in *Tsc2*$^{+/-}$ mice exacerbates vocal communication deficits that are rescued by IFNAR1$^{-/-}$

It has been previously reported that the *Tsc2*$^{+/-}$ genotype alone creates a vocal communication deficit in mouse pups (*45*, *46*), specifically a reduced rate of ultrasonic vocalizations (USVs) in *Tsc2*$^{+/-}$ compared to WT littermates at P6 (*45*). We replicated this finding and then characterized the entire call repertoire of both WT and *Tsc2*$^{+/-}$ at this time point (Fig. 9B). When we statistically compared the two groups, we found that *Tsc2*$^{+/-}$ pups exhibited an increase in the amount of short calls, chevron, and complex call types. A decrease in two-syllable calling was also observed. These results, taken together, suggest that the Tsc2 heterozygous status affects the USV pup calling pattern both quantitatively (amount of calling) and qualitatively (types of calls), leading to a call repertoire that is different than WT.

To determine whether early immune activation exacerbates vocal phenotypes in *Tsc2*$^{+/-}$ male mice, we then looked at USVs in P6 pups after a single Poly I:C injection at P3. The P6 time point was chosen because vocalizations peak in WT pups at this age and this time point allows for acute recovery from injection at P3 (*47*, *48*). Disruption of USV calling patterns is thought to model communication deficits in ASD (*46*, *49*). USVs can be classified into different call types based on their spectral features (*50*). There are more simple call types: short, upward, downward, and flat, where a single harmonic frequency is present. Simple call types are not preferred by dams, leading to decreased retrieval, and, thus, may be maladaptive (*51*). In contrast, more elaborate call types—harmonic, two syllable, complex, and chevron—have multiple harmonic frequencies, shift greatly, have breaks, are dam-preferred, and elicit retrieval.

Poly I:C–treated *Tsc2*$^{+/-}$ pups, but not their WT littermates, show a call repertoire dominated by the short call type and exhibit a significant increase in calls with an abnormal harmonic structure that does not fit into any predefined call type, referred to as

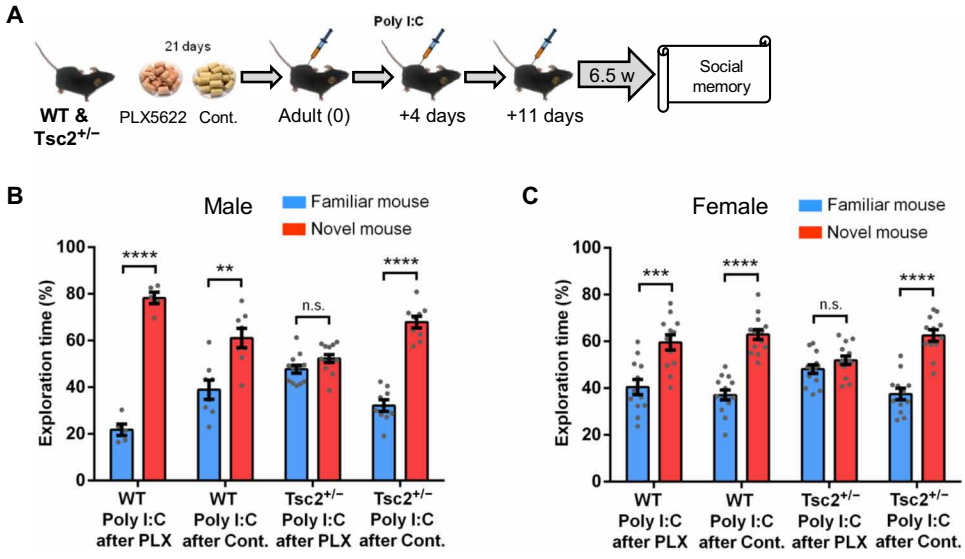

Fig. 4. Repopulation of microglia reopens a window of sensitivity to immune activation in adult male and female *Tsc2*$^{+/-}$ mice. (**A**) Timeline for injections of Poly I:C, treatment with PLX5622 (PLX; depletes microglia) or control chow and behavior approach. (**B**) Male WT/Poly I:C mice after PLX ($n = 5$; $P < 0.0001$, $t = 16.16$), WT/Poly I:C mice after control chow ($n = 8$; $P < 0.01$, $t = 1.93$), and *Tsc2*$^{+/-}$/Poly I:C mice after control chow ($n = 9$; $P < 0.0001$, $t = 10.24$), but not *Tsc2*$^{+/-}$/Poly I:C mice after PLX ($n = 13$; $P = 0.06$, $t = 1.93$), show normal social memory. Two-way ANOVA analyses using time spent exploring the novel mouse as the dependent variable revealed a significant treatment × genotype interaction [$F(1,31) = 33.55$, $P < 0.0001$], and Sidak post hoc test revealed a simple main effect of genotype on the Poly I:C after PLX group ($P < 0.0001$, $t = 6.24$). (**C**) Female WT/Poly I:C mice after PLX ($n = 12$; $P < 0.001$, $t = 4.13$), WT/Poly I:C mice after control chow ($n = 14$; $P < 0.0001$, $t = 8.72$), and *Tsc2*$^{+/-}$/Poly I:C mice after control chow ($n = 12$; $P < 0.0001$, $t = 7.27$), but not *Tsc2*$^{+/-}$/Poly I:C mice after PLX ($n = 14$; $P = 0.15$, $t = 1.47$), show normal social memory. Two-way ANOVA analyses using time spent exploring the novel mouse as the dependent variable revealed a main effect of treatment [$F(1,48) = 8.45$, $P = 0.005$], and Sidak post hoc test revealed a significant difference between *Tsc2*$^{+/-}$/Poly I:C after PLX and *Tsc2*$^{+/-}$/Poly I:C after control chow ($P < 0.01$, $t = 3.11$). Data represent means ± SEM as well as values for individual mice. Cont., control.

miscellaneous (Fig. 9C). We also observed significant decrease in the amount of harmonic calls observed in Poly I:C–treated *Tsc2*$^{+/-}$ pups compared to Poly I:C–treated WT pups. These findings, taken together, suggest a restricted vocal repertoire that is simplified and may parallel early ASD social communication deficits (see Materials and Methods for more details).

The IFNAR1$^{-/-}$ mutation rescues the abnormal neonatal vocalization pattern described above for *Tsc2*$^{+/-}$ mice injected with Poly I:C (Fig. 9D). Here, we found no difference in the amount of short or miscellaneous calling between Poly I:C–treated *Tsc2*$^{+/-}$ and WT pups. Furthermore, the harmonic call pattern is rescued by the IFNAR1$^{-/-}$ mutation, which also drives a significant increase in harmonic calling for *Tsc2*$^{+/-}$ pups when compared to WT pups. Poly I:C–treated IFNAR1$^{-/-}$/*Tsc2*$^{+/-}$ pups also exhibit a decrease in complex, upward, and frequency step call types and an increase in flat and double call types. These results demonstrate a role of type I IFN signaling in the social phenotypes of *Tsc2*$^{+/-}$ mice.

The clinical history of hospitalizations due to infections during early childhood can predict a future diagnosis of ASD

To determine whether immune activation during later stages of development could also contribute to social and other behavioral phenotypes in human ASD populations, we determined whether hospitalizations due to infections during early childhood contribute to the severity and range of phenotypes in ASD. We analyzed the clinical history of 3,575,462 children. The children were included into this analysis if they were enrolled in the claims database since their birth until at least 5 years of age, of 151 million unique Americans represented in the MarketScan dataset. Of these nearly 3.6 million children, 4417 females and 18,232 males were diagnosed with ASD. Hospitalizations due to infections significantly differentiate two populations in boys (Fig. 10A), but not in girls (Fig. 10B): the control population (boys who did not get an ASD diagnosis in the future) and boys who, at some point in the future, were diagnosed with ASD. The male population diagnosed with ASD showed a higher prevalence of infections requiring hospitalization from 1.5 to 4 years old, compared to the control population (Fig. 10A), a result consistent with the idea that strong immune activation in later stages (e.g., postnatal) of development could contribute to ASD phenotypes. Our human findings suggest that the interaction between genetic mutations and immune activation may have a far wider clinical impact than just social memory deficits in TSC2 and, instead, may be a general principle underlying a number of phenotypes in psychiatric disorders.

DISCUSSION

Here, we report a set of convergent findings that demonstrate that early postnatal microglia development is a particularly sensitive period for the ability of strong immune activation to trigger social memory deficits in *Tsc2*$^{+/-}$ male mice, a finding that our human studies suggest has clinical implications. Poly I:C injections could have affected other cell types, such as astrocytes, in addition to microglia. However, the results that we presented demonstrate that microglia play a critical role in the phenotypes described: (i) RNA-seq analysis showed a long-lasting up-regulation in microglia genes (Fig. 2B). (ii) The depletion of microglia is sufficient to permanently rescue the social memory deficits that Poly I:C injections early

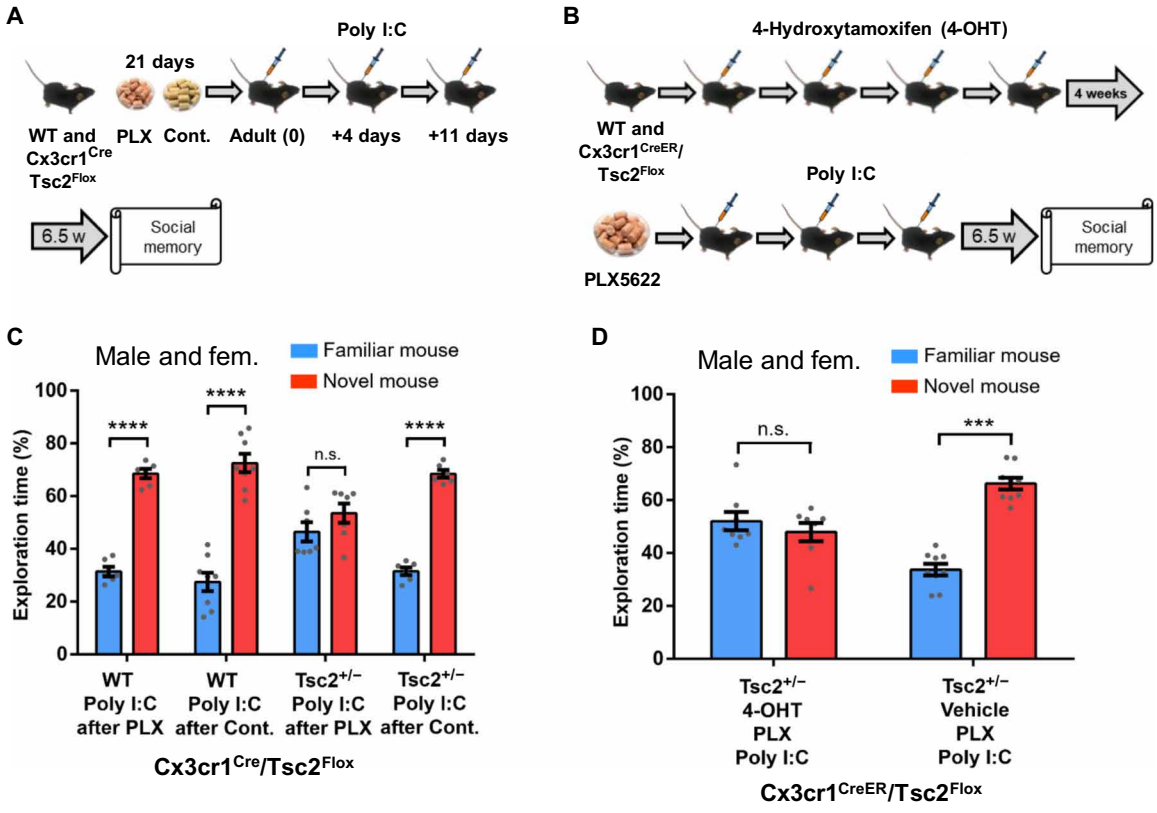

Fig. 5. Evidence for the critical role of microglia in the social memory deficits of *Tsc2*$^{+/-}$ mice with postnatal immune activation during adult microglia repopulation. (**A**) Timeline for injections of Poly I:C, treatment with PLX5622 (PLX; depletes microglia) or control chow and behavior approach. (**B**) Timeline for injections of 4-hydroxytamoxifen (4-OHT) or vehicle and Poly I:C, treatment with PLX, and behavior procedures. (**C**) Male and female WT/Poly I:C mice after PLX ($n = 6$; $P < 0.0001$, $t = 14.66$), WT/Poly I:C mice after control chow ($n = 8$; $P < 0.0001$, $t = 9.04$), and Cx3cr1^{Cre}/Tsc2^{Flox} (*Tsc2*$^{+/-}$) Poly I:C mice after control chow ($n = 6$; $P < 0.0001$, $t = 17.66$), but not Cx3cr1^{Cre}/Tsc2^{Flox} (*Tsc2*$^{+/-}$) Poly I:C mice after PLX ($n = 7$; $P = 0.19$, $t = 1.37$), show normal social memory. Two-way ANOVA analyses using time spent exploring the novel mouse as the dependent variable revealed a significant effect of treatment ($F(1,23) = 9.63$, $P = 0.005$), and Sidak post hoc test revealed a significant difference between Cx3cr1^{Cre}/Tsc2^{Flox} (*Tsc2*$^{+/-}$)/Poly I:C mice after PLX and Cx3cr1^{Cre}/Tsc2^{Flox} (*Tsc2*$^{+/-}$)/Poly I:C mice after control chow ($P < 0.01$, $t = 3.42$). (**D**) Male and female Cx3cr1^{CreER}/Tsc2^{Flox}/vehicle mice injected with Poly I:C after PLX ($n = 9$; $P < 0.0001$, $t = 10.38$), but not Cx3cr1^{CreER}/Tsc2^{Flox}/4-OHT mice injected with Poly I:C after PLX ($n = 8$; $P = 0.40$, $t = 0.84$), show normal social memory. Data represent means ± SEM as well as values for individual mice. As indicated, in (C), *Tsc2*$^{+/-}$ represents Cx3cr1^{Cre}-Tsc2^{Flox}. In (D), *Tsc2*$^{+/-}$ represents Cx3cr1^{CreER}/Tsc2^{Flox}.

postnatally induced in *Tsc2*$^{+/-}$ male mice (Fig. 3). (iii) The repopulation of microglia in adult male and female *Tsc2*$^{+/-}$ mice, following the depletion of microglia (with PLX5622), reopened a developmental window when the administration of Poly I:C was able to recreate the social memory deficits in both male and female *Tsc2*$^{+/-}$ mice (Fig. 4, B and C); these social memory deficits can themselves also be rescued with the depletion of microglia (fig. S6, B and C). (iv) The Tsc2 mutation restricted to microglia in two different mouse models together with Poly I:C activation is sufficient to recreate the social memory deficits of the Tsc2 mice (Fig. 5, C and D). These four very different lines of convergent evidence demonstrate that microglia are both necessary and sufficient for the social memory deficits of the Tsc2 mice triggered by immune activation. Our findings demonstrate a critical role for mTOR and type I IFN signaling in microglia in these memory deficits because, in addition to what we mentioned above, we were also able to rescue these deficits by deleting microglia in the adult brain, as well as with manipulations that either decreased mTOR function or specifically deleted the IFNAR1 gene. It is important to note that there are a number of published studies that support a role for microglia in neuropsychiatric phenotypes; for example, individuals diagnosed with neuropsychiatric disorders, such as ASD, have been shown to have dysfunctional microglia (*52*–*56*), and transcriptomic analyses of postmortem brain have implicated this cell type in ASD (*36*, *57*–*60*). In addition, functional genomic studies have demonstrated dysregulation of IFN signaling in ASD (*59*).

Immune activation is known to cause a number of different phenotypes in models of psychiatric disorders, including schizophrenia (*50*, *61*). However, unlike the schizophrenia models referenced above, our Tsc2 mice with early postnatal immune activation do not show deficits in social interaction (Fig. 1B and figs. S1B, S7C, and S7D) and instead show deficits in social memory (Figs. 1C, 4, and 6B). We propose that the Poly I:C injection during early postnatal development (or during the repopulation of microglia in our adult experiments) triggers an exacerbated production of IFNβ (see Fig. 7C) in the *Tsc2*$^{+/-}$ mice caused by their elevated levels of mTOR (*62*, *63*). Then, IFNβ activates IFNAR1, which, in turn, activates the mTOR pathway, and consequently triggers even more IFN production. This cycle (fig. S8) is perpetuated in microglia (deleting this cell type reverses the social memory deficits). In remarkable support of this model, blocking this cycle in adults with rapamycin permanently rescues the social memory deficits of the *Tsc2*$^{+/-}$ Ep mice. Thus, our results strongly

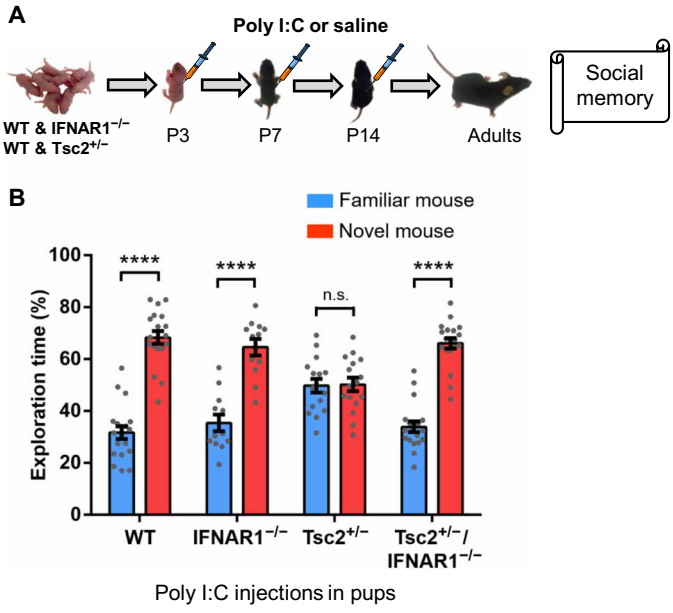

Fig. 6. A null homozygous mutation of type I IFN receptor (IFNAR1$^{-/-}$) prevents the social memory deficits of *Tsc2*$^{+/-}$ Ep mice. (**A**) Timeline for injections of Poly I:C or saline and behavior approach. (**B**) *Tsc2*$^{+/-}$ mice ($n = 16$; $P = 0.895$, $t = 0.132$) show social memory deficits. *Tsc2*$^{+/-}$/IFNAR1$^{-/-}$ mice ($n = 19$; $P < 0.0001$, $t = 11.125$), WT mice ($n = 19$; $P < 0.0001$, $t = 10.58$), and IFNAR1$^{-/-}$ mice ($n = 12$; $P < 0.0001$, $t = 6.42$) show normal social memory. Two-way ANOVA analyses using time spent exploring the novel mouse as the dependent variable revealed a significant Tsc2 × IFNAR1 genotype interaction [$F(1,62) = 14.55$, $P = 0.0003$], and Sidak post hoc test revealed a simple main effect of IFNAR genotype on the *Tsc2*$^{+/-}$ group ($P < 0.0001$, $t = 4.56$). Data represent means ± SEM as well as values for individual mice.

support a key role for this mechanism in the social memory deficits that we found. These results are consistent with recent findings that show that type I IFN can disrupt cognitive function (*64*–*66*).

Our findings provide evidence for the idea that severe (i.e., requiring hospitalization) infections in later stages of development (e.g., early postnatally) could contribute to the development of ASD. In addition, our results provide the first detailed mechanisms for how immune activation during these later stages of development coupled to genetic susceptibility could contribute to social memory and communication deficits and that these phenotypes could be prevented or even permanently reversed with drugs that target mTOR and IFNβ signaling.

MATERIALS AND METHODS

The Chancellor's Animal Research Committee at the University of California, Los Angeles approved the research protocols used here.

Experimental design and subject details

Tsc2$^{+/-}$ *mice*

To test the impact of immune activation during early postnatal development on *Tsc2*$^{+/-}$ mice, we first crossed male *Tsc2*$^{+/-}$ mice (*62*) with female WT mice. *Tsc2*$^{+/-}$ male breeders were on a C57BL/6Ncrl genetic background (Charles River Laboratories, catalog no. 027). We used C57BL/6J females [the Jackson Laboratory (JAX), catalog no. 000664] to generate experimental mice. Pregnant females were single-housed and left undisturbed except for weekly cage changes. Pregnancy was determined by checking for abdominal distension. For all the mice studied here, pregnant females were checked every day to determine the exact day when the pups were born (designated as P0). Pups were injected intraperitoneally with either Poly I:C

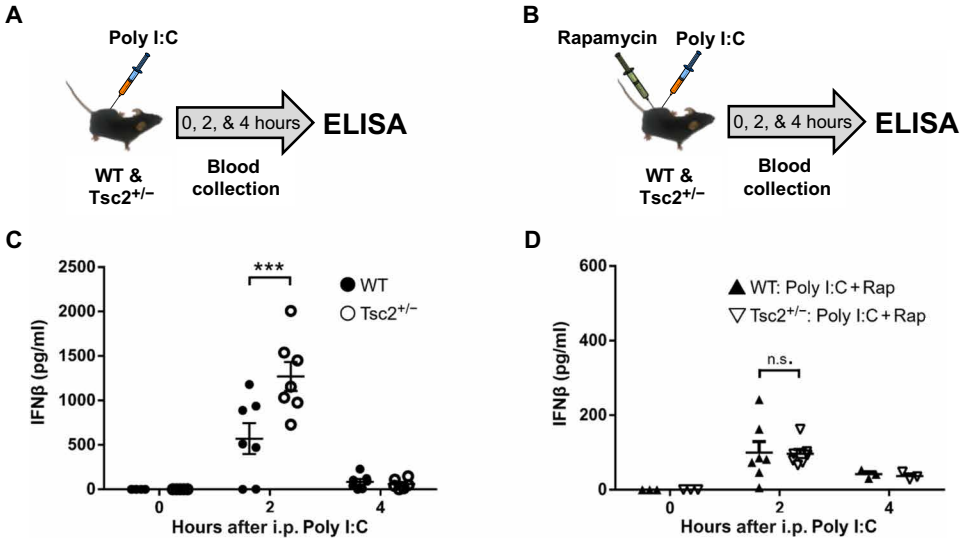

Fig. 7. Role of mammalian target of rapamycin in the increased production of IFNβ in *Tsc2*$^{+/-}$ mice caused by postnatal immune activation. (**A**) Time points of blood collection after Poly I:C injection. ELISA, enzyme-linked immunosorbent assay. (**B**) Time points of blood collection after Poly I:C and rapamycin (Rap) injection. (**C**) *Tsc2*$^{+/-}$/Poly I:C mice show significantly higher levels of serum IFNβ compared to WT/Poly I:C mice ($P < 0.001$, $t = 4.75$) 2 hours after Poly I:C injection. There is no difference in serum IFNβ levels between *Tsc2*$^{+/-}$/Poly I:C and WT/Poly I:C mice immediately ($P > 0.05$, $t = 0.00$) or 4 hours ($P > 0.05$, $t = 0.163$) after Poly I:C injection. (**D**) There is no difference in serum IFNβ levels between WT/Poly I:C + Rap and *Tsc2*$^{+/-}$/Poly I:C + Rap mice immediately ($P > 0.05$, $t = 0.00$), 2 hours ($P > 0.05$, $t = 0.73$), or 4 hours ($P > 0.05$, $t = 0.06$) after the injections. Numbers of mice used in (C) were as follows: 6 (WT/Poly I:C, 0 hours), 5 (*Tsc2*$^{+/-}$/Poly I:C, 0 hours), 7 (WT/Poly I:C, 2 hours), 7 (*Tsc2*$^{+/-}$/Poly I:C, 2 hours), 7 (WT/Poly I:C, 4 hours), and 6 (*Tsc2*$^{+/-}$/Poly I:C, 4 hours). Numbers of mice used in (D) were as follows: 3 (WT/Poly I:C + Rap, 0 hours), 7 (*Tsc2*$^{+/-}$/Poly I:C + Rap, 0 hours), 7 (WT/Poly I:C + Rap, 2 hours), 7 (*Tsc2*$^{+/-}$/Poly I:C + Rap, 2 hours), 3 (WT/Poly I:C + Rap, 4 hours), and 3 (*Tsc2*$^{+/-}$/Poly I:C + Rap, 4 hours).

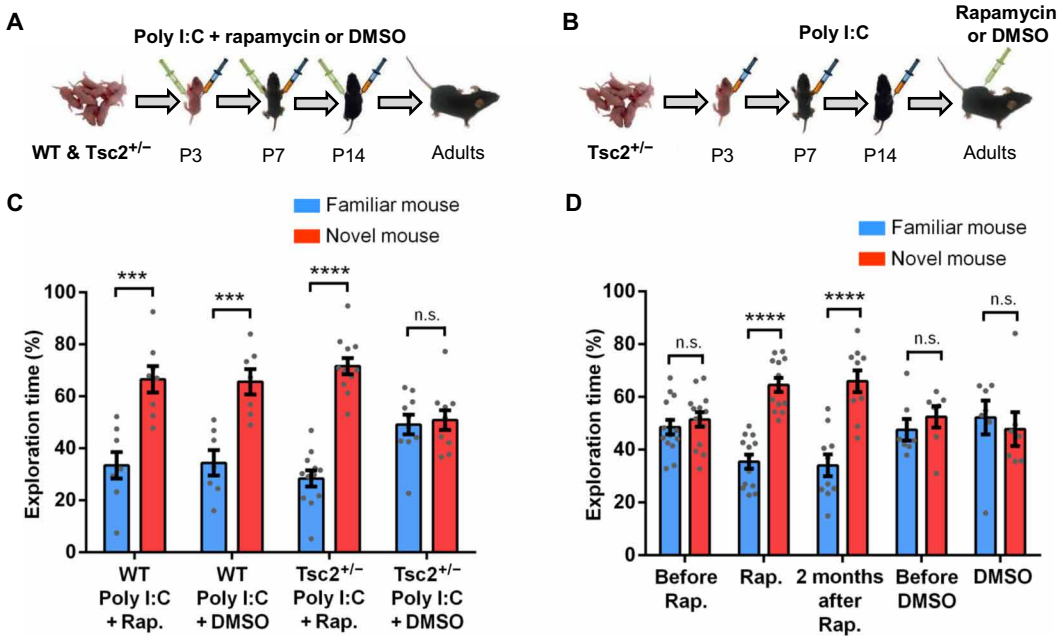

Fig. 8. Role of mTOR in the social memory deficits of *Tsc2*$^{+/-}$ Ep mice. (**A** and **B**) Timeline for injections of Poly I:C and treatment with rapamycin (Rap) or dimethyl sulfoxide (DMSO). (**C**) WT/Poly I:C + Rap ($n = 8$; $P = 0.0004$, $t = 4.60$), WT/Poly I:C + DMSO ($n = 7$; $P = 0.0007$, $t = 4.50$), and *Tsc2*$^{+/-}$/Poly I:C + Rap ($n = 12$; $P < 0.0001$, $t = 9.89$) mice show normal social memory. *Tsc2*$^{+/-}$/Poly I:C + DMSO ($n = 10$; $P = 0.758$, $t = 0.31$) mice show social memory deficit. Two-way ANOVA analyses using time spent exploring the novel mouse as the dependent variable revealed a significant treatment × genotype [$F(1,33) = 5.71$, $P = 0.02$] interaction, and Sidak post hoc test revealed a simple main effect of genotype on the Poly I:C + DMSO group ($P < 0.05$, $t = 2.42$). (**D**) *Tsc2*$^{+/-}$ mice, before rapamycin ($n = 14$; $P = 0.462$, $t = 0.74$) treatment, show social memory deficits. *Tsc2*$^{+/-}$ mice during rapamycin treatment ($n = 13$; $P < 0.0001$, $t = 7.72$) and *Tsc2*$^{+/-}$ mice 2 months after rapamycin treatment ($n = 10$; $P < 0.0001$, $t = 5.42$) show normal social memory. In contrast, *Tsc2*$^{+/-}$ mice before DMSO ($n = 7$; $P = 0.409$, $t = 0.85$) and during DMSO treatment ($n = 7$; $P = 0.63$, $t = 0.48$) show social memory deficit. Repeated-measures two-way ANOVA analyses using time spent exploring the novel mouse as the dependent variable revealed a main effect of treatment [$F(1,18) = 6.35$, $P = 0.02$], and Sidak post hoc test revealed a significant difference between *Tsc2*$^{+/-}$/Poly I:C before and after rapamycin treatment ($P < 0.05$, $t = 2.45$). Data represent means ± SEM as well as individual data points.

(20 mg/kg; Sigma-Aldrich, St. Louis, MO, USA; potassium salt; Poly I:C is supplied at 10% of the total weight of the salt; dosage was based on the weight of Poly I:C itself) or vehicle only (0.9% sterile saline) at P3, P7, and P14. To test the effect of immune activation in adult *Tsc2*$^{+/-}$ mutants, adult WT and mutant mice were injected three times with Poly I:C (20 mg/kg) following a similar relative schedule as that used during early postnatal development. Tail biopsies for genotyping were taken around P40.

IFNAR1$^{-/-}$*/Tsc2*$^{+/-}$ *mice*

To test the importance of type I IFNα and IFNβ for the phenotype that we observed in *Tsc2*$^{+/-}$ Ep mice, we generated mice that included both the *Tsc2*$^{+/-}$ and IFNAR1$^{-/-}$ null mutations by crossing *Tsc2*$^{+/-}$ male breeders with IFNAR1$^{-/-}$ females (bred on a C57Bl/6J background) for three generations (F3). These mice, together with controls, were injected early postnatally with either Poly I:C or saline at P3, P7, and P14 (see above). Tail biopsies for genotyping were taken around P40.

Cx3cr1^{Cre}*-Tsc2*^{Flox} *mice*

To confirm whether microglia play a critical role in the social memory deficits that *Tsc2*$^{+/-}$ mice show after postnatal immune activation, we crossed Cx3cr1^{Cre} mice (JAX, stock no. 025524) with Tsc2^{Flox} mice (JAX, stock no. 027458) to generate mice that carry the Tsc2 mutation only in microglia. The experimental mice were injected three times with Poly I:C (20 mg/kg) during microglia repopulation in adults (after a 21-day treatment with PLX5622) with a similar relative schedule as that used during early postnatal development. Tail biopsies for genotyping were taken around P40.

Cx3cr1^{CreER}*-Tsc2*^{Flox} *mice*

We used this mouse model to test whether heterozygous deletion of the Tsc2 gene in microglia, specifically in adult mice, was sufficient to recreate the vulnerability to postnatal immune activation. We crossed *Cx3Cr1*^{CreER} mice expressing tamoxifen-inducible Cre recombinase (JAX, stock no. 021160) with Tsc2^{Flox} mice (JAX, stock no. 027458) to generate mice that carry the *Tsc2*$^{+/-}$ mutation only in microglia of adults. The experimental mice were injected intraperitoneally with 4-OHT (Sigma-Aldrich, catalog no. H6278; 50 mg; 75 mg/kg) once per day during four consecutive days. Four weeks after the last injection of 4-OHT, the experimental mice were injected three times with Poly I:C (20 mg/kg) during microglia repopulation in adults (after a 21-day treatment with PLX5622) with a similar relative schedule as that used for the early postnatal experiments. Tail biopsies for genotyping were taken around P40.

Method details

Social interaction test

Behavioral experiments were conducted in 4- to 8-month-old mice. Crawley's three-chamber test for sociability and preference for social novelty was performed as described previously (*67*). Before the test, mice were handled for 8 min daily for six consecutive days. Then, in the next 2 days, they were habituated in an open field (63.6 cm by

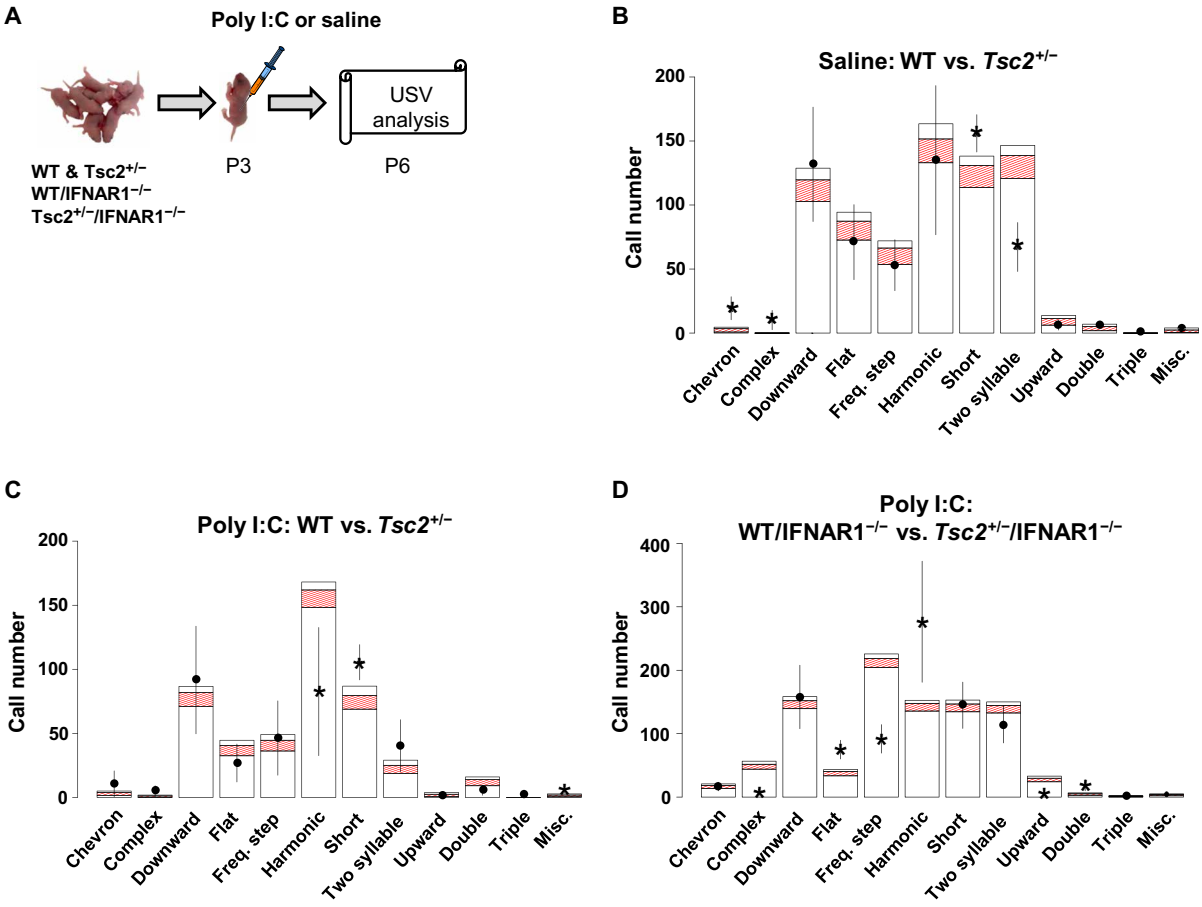

Fig. 9. A null homozygous mutation of type I IFN receptor (IFNAR1$^{-/-}$) prevents the changes in USV patterns of *Tsc2*$^{+/-}$ Ep pups. (**A**) Timeline for injections of Poly I:C or saline and behavior approach. (**B**) Comparative USV call data for saline-treated WT pups ($n = 9$) shown as bars for each call type with a 95% confidence interval in red indicating the number of calls and saline-treated *Tsc2*$^{+/-}$ pups ($n = 9$) shown as floating lines. Significance is reached for short, chevron, and complex all types (increased in *Tsc2*$^{+/-}$), and also for two-syllable (deceased in *Tsc2*$^{+/-}$). (**C**) Comparative USV call data for Poly I:C–treated WT pups ($n = 3$) shown as bars for each call type with a 95% confidence interval in red indicating number of calls and Poly I:C–treated *Tsc2*$^{+/-}$ pups ($n = 8$) shown as floating lines. Poly I:C–treated *Tsc2*$^{+/-}$ pups make significantly less harmonic calls but more short and miscellaneous calls when compared to Poly I:C–treated WT pups. (**D**) Poly I:C–treated *Tsc2*$^{+/-}$/IFNAR1$^{-/-}$ mice ($n = 12$) show no differences in the amount of short and miscellaneous call types compared to the WT/IFNAR1$^{-/-}$ Poly I:C mice ($n = 8$). Poly I:C–treated *Tsc2*$^{+/-}$/IFNAR1$^{-/-}$ mice show an increase in harmonic calling when compared to Poly I:C–treated WT/IFNAR1$^{-/-}$ mice. Other observable changes for Poly I:C–treated *Tsc2*$^{+/-}$/IFNAR1$^{-/-}$ mice include a decrease in complex, frequency step, and upward call types, and also an increase in flat and double call types.

43 cm by 24.5 cm; Plexiglas) divided into three equally sized interconnected chambers (left, center, and right) for 12 min. On the test day, an ovariectomized female (JAX, catalog no. 000691) was placed in the right or left compartment in a wire cup ("social cup"), while the other side contained an empty wire cup ("empty cup"). The test subject was released into the center compartment and allowed to freely explore the three compartments of the open field for 10 min. The exploration time was recorded during the test. Location of the social cup in the left or right chamber during the test was counterbalanced between trials. The three-chamber apparatus was cleaned after each session. Sessions were video-recorded, and social exploration time was scored offline by one to two blinded and experienced observers using stopwatches. Usually, the variation between observers was minor (0 to 3 s in the 10-min exploration sessions). Exploration was counted only when the test mouse touched with its nose either the empty cup, the social cup, or the ovariectomized female. All experiments and scoring were carried out blind to genotype and treatment condition.

Social memory test

Twenty-four hours after the SIT, mice were tested for social memory. This test involved the previously presented ovariectomized female (familiar mouse) located in the same chamber (left or right) as during training (SIT) and a new ovariectomized female (novel mouse) located in the cup that was empty during training. The test subject was released into the center compartment and allowed to freely explore the three-compartment open field for 10 min. The exploration time was recorded during this test as described above. Location of the new mouse in the left or right chamber during the test was counterbalanced between trials attending to the location of the familiar ovariectomized female during training, such that the location of the familiar ovariectomized female was always the same between training and test. The three-chamber apparatus was cleaned after each session. Sessions were video-recorded and scored offline as described above. As described above, experiments and scoring were carried out blind to genotype and treatment condition.

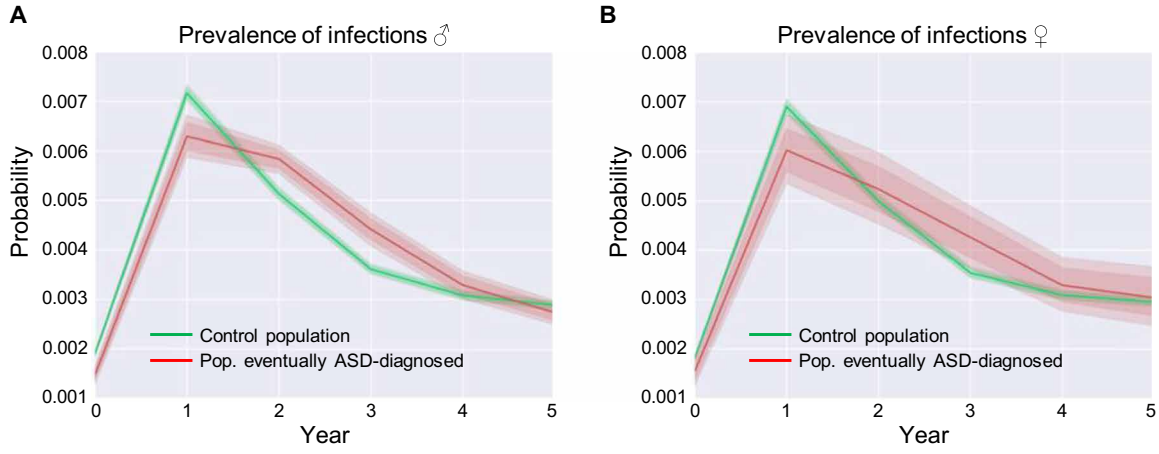

Fig. 10. Prevalence of hospitalizations due to infections in early childhood predicts the development of ASD in humans. (**A**) Probability of contracting an infection associated with hospitalization for male children over time. (**B**) Probability of contracting an infection for female children requiring hospitalization over time. (A and B) Before 1.5 years of age, infections associated with hospitalization are more prevalent in the control group, and after that, they are more prevalent in the group that, at a future time, are diagnosed with ASD. Infections associated with hospitalization significantly differentiate two population in males (A) but not in females (B): the control population (children who do not get ASD at a future time) and a population of children who, at some point in future, are diagnosed with ASD. The number of individuals in (A) was 200,552 (male). The number of individuals in (B) was 48,576 (female).

Novel object recognition test

The novel object recognition test was carried out as described previously (*68*). Twenty-four hours after the social memory test, mice were habituated in an open field (41.5 cm by 41.5 cm by 40.5 cm) for 2 days for 12 min. During the training session, mice were placed back in the open field, this time with two identical objects, and they were allowed to explore freely for 7 min. After a 24-hour interval, mice were tested for object memory with the previously presented object and a new object. Location of the new object during the test was counterbalanced between trials. Mice were trained or tested in any test only once per day. The open field was cleaned after each session. Sessions were video-recorded and scored offline as described above. The variation between observers was normally less than 2 s in the 7-min exploration sessions. Exploration was counted only when the test mouse touched the objects with its nose. All experiments and scoring were carried out blind to genotype and treatment condition. The objects included in this study were small bottles or containers of different shapes.

Recording and analysis of pup ultrasonic isolation vocalizations

Mouse pups were removed from the nest, four at a time, and individually placed into sound attenuation chambers for recording. Pups were then recorded in isolation for 15 min. All dams were WT except in the case of the IFNAR1$^{-/-}$ pups, where *Tsc2*$^{+/-}$ dams were included. An ultrasonic microphone (CM16; Avisoft Bioacoustics, Nordbahn, Germany) was suspended through a hole in the top of the chamber and recorded calls. Microphones were connected to a recording device (UltraSoundGate 416Hb, Avisoft Bioacoustics) allowing for transduction to spectrograms for further analysis (Avisoft SASLab Pro). Recordings were conducted at P6. After the P6 recording session, each pup was tattooed to enable identification for later recording and genotyping procedures. Pups were recorded within the same 2-hour time window each day (light: 10:00 a.m. to 12:00 p.m.) to control for circadian effects. Temperature was maintained at 21° to 22°C. USVs were segmented using an in-house MATLAB code and then classified using Vocal Inventory Clustering Engine (VoICE) as previously described (*69*).

Call types were classified according to Scattoni and colleagues (*70*), and in the case of rapid succession of calls (<10 ms between calls), the "double" and "triple" call types were added to our categorization schema. The "miscellaneous" category includes all highly abnormal call types that do not fit into any other categorization. For statistical analyses, see section below.

Poly I:C administration

We freshly dissolved Poly I:C potassium salt (Sigma-Aldrich, catalog no. P9582-50MG; Poly I:C is supplied at 10% of the total weight of the salt; dosage was based on the weight of Poly I:C itself) in vehicle solution (0.9% sterile saline) before use.

Early postnatal administration. *Tsc2*$^{+/-}$ and WT mice were injected intraperitoneally with Poly I:C (20 mg/kg) or vehicle at P3, P7, and P14.

Administration 2 hours before social memory test. Adult (4 to 6 months) *Tsc2*$^{+/-}$ and WT littermates were injected intraperitoneally with either Poly I:C (20 mg/kg) or vehicle at 4 months, 4 days, 11 days, and 12 days later.

Administration 8 weeks before social memory test. Adult (~4 months) *Tsc2*$^{+/-}$ and WT littermates were injected intraperitoneally with either Poly I:C (20 mg/kg) or vehicle at 4 months, 4 days, and 11 days later.

Administration during repopulation of microglia in adult mice. Adult (4 to 6 months) *Tsc2*$^{+/-}$ and WT littermates were fed with PLX5622 or control chow during 21 days (see the "PLX5622 treatment" section for more details). The mice were injected intraperitoneally with Poly I:C (20 mg/kg) 10 hours, 4 days, and 11 days after the treatment with PLX5622 or control chow.

Rapamycin treatment

We freshly dissolved rapamycin (5 mg/kg; LC Laboratories, catalog no. R-5000) in vehicle solution [100% dimethyl sulfoxide (DMSO); Sigma-Aldrich, catalog no. D5879-500ML] before use.

Adult treatment. *Tsc2*$^{+/-}$ mice were injected with Poly I:C at P3, P7, and P14. As adults (4 to 6 months), those mice were treated with a single intraperitoneal injection of rapamycin (5 mg/kg) or vehicle (DMSO) daily for 5 days before the social memory test. Mice were

tested for social memory 18 hours after the last injection of rapamycin or DMSO as well as 2 months after that.

Early postnatal treatment. $Tsc2^{+/-}$ and WT mice were injected simultaneously with Poly I:C (20 mg/kg) and rapamycin (5 mg/kg) or DMSO at P3, P7, and P14. As adults (4 to 6 months), those mice were tested for social interaction and, the next day, for social memory as described above.

PLX5622 treatment

PLX5622 and control rodent diet was provided by Plexxikon Inc. and formulated in AIN-76A standard chow by Research Diets Inc. at the doses indicated below.

PLX5622 treatment in mice injected with Poly I:C early postnatally. We injected $Tsc2^{+/-}$ mice with Poly I:C (20 mg/kg) at P3, P7, and P14. As adults (4 to 6 months), those mice were fed with PLX5622 (1200 mg/kg; catalog no. D11100404i) or control chow (catalog no. D10001i) for 21 days (*71*). At day 21 of PLX treatment, mice were tested for social interaction and, 24 hours later, for social memory. Mice were tested again, 2 months after the last day of PLX treatment, for social interaction and, the next day, for social memory.

PLX treatment in adult mice that were not injected with Poly I:C early postnatally. Adult (4 to 6 months old) WT and $Tsc2^{+/-}$ mice were fed with PLX5622 (1200 mg/kg) or control chow for 21 days (5 g of chow per mouse per day). The mice were then injected with Poly I:C (20 mg/kg) at 10 hours, 4 days, and 11 days after the last PLX or control chow treatment. Two months later, mice were tested for social interaction and, 24 hours later, for social memory as described above.

4-OHT treatment

A solution of 4-OHT was prepared using pure ethanol (Sigma-Aldrich, catalog no. E7023-1L) and corn oil (Sigma-Aldrich, catalog no. C8267-500ML). First, we added the 4-OHT (125 mg/ml; Sigma-Aldrich, catalog no. H6278-50 mg) to ethanol (100%; pure) and incubated this solution at 55°C with vortexing for 15 min. Then, corn oil was added to a final concentration of 4-OHT (12.5 mg/ml). Adult experimental mice were injected intraperitoneally with either 4-OHT (75 mg/kg) or vehicle once a day for four consecutive days.

Kinetic analysis of IFNβ and protein quantification

Adult (4 to 6 months old) $Tsc2^{+/-}$ and WT littermate mice received a single intraperitoneal injection of Poly I:C (20 mg/kg). Blood was collected by retro-orbital puncture. Serum was separated from clotted blood by centrifugation. Serum IFNβ was measured using the Verikin Mouse IFN-Beta ELISA (PBL Assay Science, Piscataway Township, New Jersey) according to the manufacturer's instructions. The concentration of sample IFNβ was determined by calculating the four-parameter fit of the standard curve. *P* values were calculated by two-way analysis of variance (ANOVA).

Immunohistochemistry

This was performed as described earlier (*72*). Briefly, mice were perfused transcardially with a fixative containing 4% paraformaldehyde and cryoprotected with 30% sucrose. Coronal and sagittal brain sections, 60 μm thick, were incubated overnight at 4°C with monoclonal rabbit anti-Iba1 (1:1000 dilutions; Wako Chemicals, catalog no. 019-19741). The sections were then incubated for 90 min with Alexa Fluor 488 goat anti-rabbit immunoglobulin G (1:500 dilutions; Invitrogen, catalog no. A11011). After that, the sections were incubated in 4′,6-diamidino-2-phenylindole (1:1000 dilutions) for 15 min and then in phosphate-buffered saline for 14 min. The immunofluorescence labeling was detected with a confocal microscope.

RNA-seq methods for $Tsc2^{+/-}$ Poly I:C brain gene expression analyses

Brain tissue from prefrontal cortex, hippocampus, and cerebellum was macrodissected and flash-frozen on dry ice. Approximately 50 to 100 mg of frozen brain tissue were then pulverized, and RNA was extracted using QIAGEN miRNeasy kits according to the manufacturer's protocol. For each sample, RNA integrity number values were quantified using an Agilent Bioanalyzer. RNA-seq libraries were prepared using TruSeq Stranded mRNA Library Prep kits following ribosomal RNA depletion using Ribo-Zero Gold (Illumina). Libraries were barcoded and randomly pooled in sets of 18. Each pool was then sequenced twice on an Illumina HiSeq 4000 with standard chemistry and protocols for 69–base pair paired-end reads to achieve an average depth of 35 million reads per sample. Demulitplexed fastq files were mapped to the mouse reference genome assembly (GRCm38/mm10) using STAR (version 2.5.2a). Quality control was performed using Picard Tools v2.6.2 (CollectAlignmnetSummaryMetrics, CollectRnaSeqMetrics, CollectGcBiasMetrics, CollectInsertSizeMetrics, and MarkDuplicates). To control for differences in RNA quality, read depth, and other sequencing-related technical artifacts across subjects, we created a matrix of "sequencing statistics" corresponding to the aggregate of above Picard Tools metrics for each sample. Two sequencing statistics, seqPC1 and seqPC2, were calculated as the first and second principal components of this matrix and were used as covariates in downstream analyses as previously published (*36*). Gene expression levels were then quantified using Kallisto with Gencode M17 annotations and compiled using the tximport package in R. Genes were filtered to retain only those with a minimum counts per million (CPM) of 1 in at least half of the samples. Outliers samples ($n = 1$) were identified from each brain region separately as those with standardized sample network connectivity Z scores < -2, as described (*73*), and were removed. Count-level data then underwent trimmed mean of m values (TMM) scale normalization, followed by voom transformation and differential gene expression using the limma package (*74*) in R. Random effects of individual subject were accounted for using the duplicateCorrelation function, controlling for the fact that several brain samples were taken from the same mouse (multiple regions, both hemispheres). Test statistics were calculated for the following contrast: $Tsc2^{+/-}$ early postnatal Poly I:C versus $Tsc2^{+/-}$ early postnatal saline. Local FDR correction was applied to account for multiple comparisons with the fdrtool package in R. Genes with FDR < 0.1 were identified as being differentially expressed. Cell type–specific enrichment analysis was performed using the GSEA function in the clusterProfiler package, using markers derived from Zhang *et al.* (*75*).

Analysis of the correlation between ASD and history of severe infections during childhood

The figures were generated in three stages: (i) From a very large health record dataset, we selected child medical histories that spanned the time interval from a child's birth to their 5-year-old age. (ii) We matched children that eventually developed ASD ("affected") with unaffected kids, using all descriptors available to us (county and sex), and then, (iii) we statistically compared these two groups of children with respect to their susceptibility to infectious versus noninfectious diseases. In the first stage, we used Truven MarketScan, an insurance claim dataset covering over half of the U.S. population to select 3,575,462 unique child histories, including 1,636,108 females and 1,939,354 males. In the second stage, we matched individual histories by sex and county to select 10 comparison unaffected individuals

for each affected individual. This way, we identified 18,232 affected male histories matched with 182,320 unaffected ones, as well as 4416 affected female histories matched with 44,160 unaffected ones. The total number of individuals under consideration thus ended up to be 249,128 (including 48,576 females and 200,552 males). The females were distributed across 979 U.S. counties, while the more numerous boys were distributed across 1749 counties.

The third stage included three steps leading to a computation of 99% confidence intervals for the probability of infectious and non-infectious diseases experienced by children in each group during each year of life. The three steps included (i) bootstrap resampling, (ii) central tendency estimation, and (iii) confidence interval determination.

The computations were conducted using the seaborn package (https://seaborn.pydata.org). To identify ASD, we used the following The International Classification of Diseases, Ninth Revision, Clinical Modification (ICD-9-CM) codes: 299.0, 299.00, 299.01, 299.9, 299.8, 299.91, 299.90, 299.80, 299.81, 299.1, 299.10, and 299.11.

To identify infections, we used the following codes: 487.8, 488.12, 488.1, 488.0, 488.01, 488.02, 487.0, 487.1, 488.19, 488.09, 488, 487, 488.11, 112.3, 112.2, 112.1, 112.0, 112.5, 112.9, 112.8, 115, 114, 117, 116, 111, 110, 112, 112.84, 112.85, 116.0, 118, 112.82, 115.09, 110.1, 111.3, 115.1, 115.00, 111.0, 110.5, 111.1, 115.90, 115.99, 115.19, 115.9, 518.6, 117.2, 117.3, 117.0, 117.1, 117.6, 117.7, 117.4, 117.5, 111.8, 117.8, 117.9, 116.2, 116.1, 111.9, 115.0, 110.0, 110.3, 110.2, 114.9, 110.4, 111.2, 110.6, 110.9, 110.8, 114.1, 115.10, 114.3, 112.89, 005.81, 005.89, 001.0, 001.1, 001.9, 003.0, 003.2, 003.8, 003.9, 008.6, 008.5, 008.4, 008.3, 008.2, 008.1, 008.0, 008.8, 003.20, 003.24, 003.29, 008.44, 008.45, 008.46, 008.47, 008.41, 008.42, 008.43, 008.49, 006.0, 006.3, 006.2, 006.5, 006.4, 006.6, 006.9, 006.8, 009.2, 009.3, 009.0, 009.1, 007.5, 007.2, 007.3, 007.9, 004.3, 004.2, 004.1, 004.0, 004.9, 004.8, 008.00, 008.01, 008.02, 008.03, 008.04, 008.09, 002.9, 021.1, 002.1, 002.0, 002.3, 002.2, 022.2, 005.4, 005.2, 005.3, 005.0, 005.1, 005.8, 005.9, 003, 002, 001, 007, 006, 005, 004, 009, 008, 008.69, 008.62, 008.63, 008.61, 008.66, 008.67, 008.64, 008.65, 041.5, 041.7, 041.9, 037, 040.3, 039, 033.1, 033.0, 041.8, 040.2, 032, 033, 040.1, 040.0, 033.9, 033.8, 041.2, 040.4, 027.2, 027.0, 027.1, 041.89, 026.9, 036, 027.8, 027.9, 041.6, 026.0, 032.89, 020.0, 020.9, 020.8, 021.8, 021.9, 032.8, 032.9, 041.84, 023.2, 023.3, 023.0, 023.1, 022.9, 022.8, 041.83, 041.82, 023.8, 023.9, 025, 024, 027, 026, 021, 020, 023, 022, 036.89, 041, 040, 036.8, 036.9, 039.9, 039.8, 041.3, 039.4, 039.3, 039.2, 036.3, 041.81, 040.8, 040.81, 040.82, 041.85, 036.81, 040.42, 040.89, 072.7, 072.0, 072.3, 072.8, 072.9, 078.3, 056.8, 056.9, 056.0, 056.7, 056.09, 056.00, 074.3, 074.0, 074.1, 074.8, 050.9, 050.0, 050.1, 050.2, 079.52, 079.51, 056.79, 079.59, 066.9, 066.8, 055.79, 079.81, 079.82, 079.83, 079.50, 079.88, 079.89, 078, 059.09, 059.00, 059.01, 051.02, 079.3, 051.01, 079.2, 059.12, 060.9, 079.99, 079.98, 060.1, 060.0, 066.3, 066.1, 066.0, 059, 066.4, 055, 056, 057, 050, 051, 059.19, 079.9, 079.8, 059.11, 059.10, 079.1, 071, 079.6, 079.5, 073.8, 061, 060, 065, 066, 059.20, 059.21, 059.22, 079, 066.40, 066.41, 074, 075, 072, 073, 073.7, 057.0, 073.9, 066.49, 057.9, 057.8, 055.7, 078.89, 078.88, 055.9, 055.8, 078.81, 072.71, 072.72, 078.6, 078.7, 078.4, 078.5, 078.2, 072.79, 078.0, 078.82, 075.0, 065.4, 065.0, 065.1, 065.2, 065.3, 065.8, 065.9, 079.0, 051.9, 078.8, 051.1, 051.0, 051.2, 059.1, 059.0, 059.2, 059.9, 059.8, 066.42.

Statistical analysis

Mouse behavioral data are presented as means ± SEM as well as individual data. For behavioral experiments, statistics presented on the figures were based on Student's *t* tests. We also analyze the data using two-way ANOVA and Holm-Sidak post hoc analyses and we obtain identical results. For the kinetic analyses of IFNβ production, two-way ANOVA was performed. *P*, *t*, and *F* values are presented in the figure legends, *n* values are provided in the figure legends. $P < 0.05$ was considered significant. $P > 0.05$, $P < 0.05$, $P < 0.01$, $P < 0.001$, and $P < 0.0001$ were denoted as n.s. (nonsignificant), *, **, ***, and ****, respectively. GraphPad Prism 7 software was used to perform statistical analyses and for generating graphical representations of the data.

To statistically assess the genotype effect on USV repertoire, we used a resampling technique, where the WT call distribution was used to generate an expected call distribution for the $Tsc2^{+/-}$ animals. The median count of each call type across WT pups was calculated and used to generate a resampling pool. From this pool, the total number of calls made by the $Tsc2^{+/-}$ pups was drawn, with replacement. The count of each call type in this resampled distribution was then stored. This process was repeated 10,000 times, generating 10,000 counts of each call type expected should the gene knockout have no effect. The 95% confidence interval was calculated for the distribution of each call type. Last, to determine statistical significance, the average count of each call type produced by the $Tsc2^{+/-}$ animals was compared to the resampled distribution. If the average count ± SEM fell outside the 95% confidence interval of the resampled data, then a statistically significant over- or underrepresentation of that call type was said to result from the change in genotype.

For RNA-seq analysis, local FDR correction was applied to account for multiple comparisons with the fdrtool package (*76*) in R. Genes with FDR < 0.1 were identified as being differentially expressed. No animals or data points were excluded from analyses.

SUPPLEMENTARY MATERIALS

Supplementary material for this article is available at https://science.org/doi/10.1126/sciadv.abf2073

View/request a protocol for this paper from *Bio-protocol*.

REFERENCES AND NOTES

1. M. L. Estes, A. K. McAllister, Maternal immune activation: Implications for neuropsychiatric disorders. *Science* **353**, 772–777 (2016).
2. European Chromosome 16 Tuberous Sclerosis Consortium, Identification and characterization of the tuberous sclerosis gene on chromosome 16. *Cell* **75**, 1305–1315 (1993).
3. M. van Slegtenhorst, R. de Hoogt, C. Hermans, M. Nellist, B. Janssen, S. Verhoef, D. Lindhout, A. van den Ouweland, D. Halley, J. Young, M. Burley, S. Jeremiah, K. Woodward, J. Nahmias, M. Fox, R. Ekong, J. Osborne, J. Wolfe, S. Povey, R. G. Snell, J. P. Cheadle, A. C. Jones, M. Tachataki, D. Ravine, J. R. Sampson, M. P. Reeve, P. Richardson, F. Wilmer, C. Munro, T. L. Hawkins, T. Sepp, J. B. Ali, S. Ward, A. J. Green, J. R. Yates, J. Kwiatkowska, E. P. Henske, M. P. Short, J. H. Haines, S. Jozwiak, D. J. Kwiatkowski, Identification of the tuberous sclerosis gene TSC1 on chromosome 9q34. *Science* **277**, 805–808 (1997).
4. P. J. de Vries, V. H. Whittemore, L. Leclezio, A. W. Byars, D. Dunn, K. C. Ess, D. Hook, B. H. King, M. Sahin, A. Jansen, Tuberous sclerosis associated neuropsychiatric disorders (TAND) and the TAND Checklist. *Pediatr. Neurol.* **52**, 25–35 (2015).
5. T. T. Gipson, G. Gerner, M. A. Wilson, M. E. Blue, M. V. Johnston, Potential for treatment of severe autism in tuberous sclerosis complex. *World J. Clin. Pediatr.* **2**, 16–25 (2013).
6. A. Vignoli, F. la Briola, A. Peron, K. Turner, C. Vannicola, M. Saccani, E. Magnaghi, G. F. Scornavacca, M. P. Canevini, Autism spectrum disorder in tuberous sclerosis complex: Searching for risk markers. *Orphanet J. Rare Dis.* **10**, 154 (2015).
7. S. E. Smith, J. Li, K. Garbett, K. Mirnics, P. H. Patterson, Maternal immune activation alters fetal brain development through interleukin-6. *J. Neurosci.* **27**, 10695–10702 (2007).
8. U. Meyer, J. Feldon, Neural basis of psychosis-related behaviour in the infection model of schizophrenia. *Behav. Brain Res.* **204**, 322–334 (2009).
9. L. Shi, S. H. Fatemi, R. W. Sidwell, P. H. Patterson, Maternal influenza infection causes marked behavioral and pharmacological changes in the offspring. *J. Neurosci.* **23**, 297–302 (2003).
10. N. V. Malkova, C. Z. Yu, E. Y. Hsiao, M. J. Moore, P. H. Patterson, Maternal immune activation yields offspring displaying mouse versions of the three core symptoms of autism. *Brain Behav. Immun.* **26**, 607–616 (2012).

11. G. B. Choi, Y. S. Yim, H. Wong, S. Kim, H. Kim, S. V. Kim, C. A. Hoeffer, D. R. Littman, J. R. Huh, The maternal interleukin-17a pathway in mice promotes autism-like phenotypes in offspring. *Science* **351**, 933–939 (2016).
12. H. O. Atladóttir, P. Thorsen, L. Østergaard, D. E. Schendel, S. Lemcke, M. Abdallah, E. T. Parner, Maternal infection requiring hospitalization during pregnancy and autism spectrum disorders. *J. Autism Dev. Disord.* **40**, 1423–1430 (2010).
13. P. H. Patterson, Immune involvement in schizophrenia and autism: Etiology, pathology and animal models. *Behav. Brain Res.* **204**, 313–321 (2009).
14. A. S. Brown, A. Sourander, S. Hinkka-Yli-Salomäki, I. W. McKeague, J. Sundvall, H. M. Surcel, Elevated maternal C-reactive protein and autism in a national birth cohort. *Mol. Psychiatry* **19**, 259–264 (2014).
15. H. O. Atladottir, M. G. Pedersen, P. Thorsen, P. B. Mortensen, B. Deleuran, W. W. Eaton, E. T. Parner, Association of family history of autoimmune diseases and autism spectrum disorders. *Pediatrics* **124**, 687–694 (2009).
16. P. Ashwood, S. Wills, J. Van de Water, The immune response in autism: A new frontier for autism research. *J. Leukoc. Biol.* **80**, 1–15 (2006).
17. B. K. Lee, C. Magnusson, R. M. Gardner, Å. Blomström, C. J. Newschaffer, I. Burstyn, H. Karlsson, C. Dalman, Maternal hospitalization with infection during pregnancy and risk of autism spectrum disorders. *Brain Behav. Immun.* **44**, 100–105 (2015).
18. C. Dalman, P. Allebeck, D. Gunnell, G. Harrison, K. Kristensson, G. Lewis, S. Lofving, F. Rasmussen, S. Wicks, H. Karlsson, Infections in the CNS during childhood and the risk of subsequent psychotic illness: A cohort study of more than one million Swedish subjects. *Am. J. Psychiatry* **165**, 59–65 (2008).
19. D. A. Rossignol, S. J. Genuis, R. E. Frye, Environmental toxicants and autism spectrum disorders: A systematic review. *Transl. Psychiatry* **4**, e360 (2014).
20. S. D. Bilbo, J. M. Schwarz, Early-life programming of later-life brain and behavior: A critical role for the immune system. *Front. Behav. Neurosci.* **3**, 14 (2009).
21. S. S. Moy, J. J. Nadler, A. Perez, R. P. Barbaro, J. M. Johns, T. R. Magnuson, J. Piven, J. N. Crawley, Sociability and preference for social novelty in five inbred strains: An approach to assess autistic-like behavior in mice. *Genes Brain Behav.* **3**, 287–302 (2004).
22. M. Zhou, S. Greenhill, S. Huang, T. K. Silva, Y. Sano, S. Wu, Y. Cai, Y. Nagaoka, M. Sehgal, D. J. Cai, Y. S. Lee, K. Fox, A. J. Silva, CCR5 is a suppressor for cortical plasticity and hippocampal learning and memory. *eLife* **5**, (2016).
23. A. Ennaceur, J. Delacour, A new one-trial test for neurobiological studies of memory in rats. 1: Behavioral data. *Behav. Brain Res.* **31**, 47–59 (1988).
24. L. K. Bicks, H. Koike, S. Akbarian, H. Morishita, Prefrontal cortex and social cognition in mouse and man. *Front. Psychol.* **6**, 1805 (2015).
25. E. L. Stevenson, H. K. Caldwell, Lesions to the CA2 region of the hippocampus impair social memory in mice. *Eur. J. Neurosci.* **40**, 3294–3301 (2014).
26. P. T. Tsai, C. Hull, Y. X. Chu, E. Greene-Colozzi, A. R. Sadowski, J. M. Leech, J. Steinberg, J. N. Crawley, W. G. Regehr, M. Sahin, Autistic-like behaviour and cerebellar dysfunction in Purkinje cell Tsc1 mutant mice. *Nature* **488**, 647–651 (2012).
27. D. Riva, C. Georgia, The contribution of the cerebellum to mental and social functions in developmental age. *Hum. Physiol.* **26**, 21–25 (2000).
28. R. M. Reith, J. McKenna, H. Wu, S. S. Hashmi, S. H. Cho, P. K. Dash, M. J. Gambello, Loss of Tsc2 in Purkinje cells is associated with autistic-like behavior in a mouse model of tuberous sclerosis complex. *Neurobiol. Dis.* **51**, 93–103 (2013).
29. F. Hoche, X. Guell, J. C. Sherman, M. G. Vangel, J. D. Schmahmann, Cerebellar contribution to social cognition. *Cerebellum* **15**, 732–743 (2016).
30. M. L. Phillips, H. A. Robinson, L. Pozzo-Miller, Ventral hippocampal projections to the medial prefrontal cortex regulate social memory. *eLife* **8**, (2019).
31. A. Pirone, J. M. Alexander, J. B. Koenig, D. R. Cook-Snyder, M. Palnati, R. J. Wickham, L. Eden, N. Shrestha, L. Reijmers, T. Biederer, K. A. Miczek, C. G. Dulla, M. H. Jacob, Social stimulus causes aberrant activation of the medial prefrontal cortex in a mouse model with autism-like behaviors. *Front. Synaptic Neurosci.* **10**, 35 (2018).
32. H. Sugimoto, T. Tsukiura, Contribution of the medial prefrontal cortex to social memory. *Brain Nerve* **70**, 753–761 (2018).
33. K. Yamashiro, K. Hori, E. S. K. Lai, R. Aoki, K. Shimaoka, N. Arimura, S. F. Egusa, A. Sakamoto, M. Abe, K. Sakimura, T. Watanabe, N. Uesaka, M. Kano, M. Hoshino, AUTS2 governs cerebellar development, purkinje cell maturation, motor function and social communication. *iScience* **23**, 101820 (2020).
34. H. Sacai, K. Sakoori, K. Konno, K. Nagahama, H. Suzuki, T. Watanabe, M. Watanabe, N. Uesaka, M. Kano, Autism spectrum disorder-like behavior caused by reduced excitatory synaptic transmission in pyramidal neurons of mouse prefrontal cortex. *Nat. Commun.* **11**, 5140 (2020).
35. M. Pagani, A. Bertero, A. Liska, A. Galbusera, M. Sabbioni, N. Barsotti, N. Colenbier, D. Marinazzo, M. L. Scattoni, M. Pasqualetti, A. Gozzi, Deletion of autism risk gene Shank3 disrupts prefrontal connectivity. *J. Neurosci.* **39**, 5299–5310 (2019).
36. N. N. Parikshak, V. Swarup, T. G. Belgard, M. Irimia, G. Ramaswami, M. J. Gandal, C. Hartl, V. Leppa, L. d. l. T. Ubieta, J. Huang, J. K. Lowe, B. J. Blencowe, S. Horvath, D. H. Geschwind, Genome-wide changes in lncRNA, splicing, and regional gene expression patterns in autism. *Nature* **540**, 423–427 (2016).
37. M. R. P. Elmore, A. R. Najafi, M. A. Koike, N. N. Dagher, E. E. Spangenberg, R. A. Rice, M. Kitazawa, B. Matusow, H. Nguyen, B. L. West, K. N. Green, Colony-stimulating factor 1 receptor signaling is necessary for microglia viability, unmasking a microglia progenitor cell in the adult brain. *Neuron* **82**, 380–397 (2014).
38. J. M. Schwarz, P. W. Sholar, S. D. Bilbo, Sex differences in microglial colonization of the developing rat brain. *J. Neurochem.* **120**, 948–963 (2012).
39. S. Yona, K. W. Kim, Y. Wolf, A. Mildner, D. Varol, M. Breker, D. Strauss-Ayali, S. Viukov, M. Guilliams, A. Misharin, D. A. Hume, H. Perlman, B. Malissen, E. Zelzer, S. Jung, Fate mapping reveals origins and dynamics of monocytes and tissue macrophages under homeostasis. *Immunity* **38**, 79–91 (2013).
40. X. Zhao, Y. Liao, S. Morgan, R. Mathur, P. Feustel, J. Mazurkiewicz, J. Qian, J. Chang, G. W. Mathern, M. A. Adamo, A. L. Ritaccio, M. Gruenthal, X. Zhu, Y. Huang, Noninflammatory changes of microglia are sufficient to cause epilepsy. *Cell Rep.* **22**, 2080–2093 (2018).
41. C. N. Parkhurst, G. Yang, I. Ninan, J. N. Savas, J. R. Yates III, J. J. Lafaille, B. L. Hempstead, D. R. Littman, W. B. Gan, Microglia promote learning-dependent synapse formation through brain-derived neurotrophic factor. *Cell* **155**, 1596–1609 (2013).
42. A. K. Field, A. A. Tytell, G. P. Lampson, M. R. Hilleman, Inducers of interferon and host resistance. II. Multistranded synthetic polynucleotide complexes. *Proc. Natl. Acad. Sci. U.S.A.* **58**, 1004–1010 (1967).
43. S. Marshall-Clarke, J. E. Downes, I. R. Haga, A. G. Bowie, P. Borrow, J. L. Pennock, R. K. Grencis, P. Rothwell, Polyinosinic acid is a ligand for toll-like receptor 3. *J. Biol. Chem.* **282**, 24759–24766 (2007).
44. W. Cao, S. Manicassamy, H. Tang, S. P. Kasturi, A. Pirani, N. Murthy, B. Pulendran, Toll-like receptor-mediated induction of type I interferon in plasmacytoid dendritic cells requires the rapamycin-sensitive PI(3)K-mTOR-p70S6K pathway. *Nat. Immunol.* **9**, 1157–1164 (2008).
45. E. A. Greene-Colozzi, A. R. Sadowski, E. Chadwick, P. T. Tsai, M. Sahin, Both maternal and pup genotype influence ultrasonic vocalizations and early developmental milestones in tsc2 (+/–) mice. *Epilepsy Res. Treat.* **2014**, 784137 (2014).
46. D. M. Young, A. K. Schenk, S. B. Yang, Y. N. Jan, L. Y. Jan, Altered ultrasonic vocalizations in a tuberous sclerosis mouse model of autism. *Proc. Natl. Acad. Sci. U.S.A.* **107**, 11074–11079 (2010).
47. J. N. Crawley, Designing mouse behavioral tasks relevant to autistic-like behaviors. *Ment. Retard. Dev. Disabil. Res. Rev.* **10**, 248–258 (2004).
48. E. Noirot, Ultra-sounds in young rodents. I. Changes with age in albino mice. *Anim. Behav.* **14**, 459–462 (1966).
49. J. N. Crawley, Mouse behavioral assays relevant to the symptoms of autism. *Brain Pathol.* **17**, 448–459 (2007).
50. P. H. Patterson, Maternal infection: Window on neuroimmune interactions in fetal brain development and mental illness. *Curr. Opin. Neurobiol.* **12**, 115–118 (2002).
51. T. Takahashi, S. Okabe, P. Ó. Broin, A. Nishi, K. Ye, M. V. Beckert, T. Izumi, A. Machida, G. Kang, S. Abe, J. L. Pena, A. Golden, T. Kikusui, N. Hiroi, Structure and function of neonatal social communication in a genetic mouse model of autism. *Mol. Psychiatry* **21**, 1208–1214 (2016).
52. G. Juckel, M. P. Manitz, M. Brüne, A. Friebe, M. T. Heneka, R. J. Wolf, Microglial activation in a neuroinflammational animal model of schizophrenia—A pilot study. *Schizophr. Res.* **131**, 96–100 (2011).
53. R. Koyama, Y. Ikegaya, Microglia in the pathogenesis of autism spectrum disorders. *Neurosci. Res.* **100**, 1–5 (2015).
54. A. Monji, T. Kato, S. Kanba, Cytokines and schizophrenia: Microglia hypothesis of schizophrenia. *Psychiatry Clin. Neurosci.* **63**, 257–265 (2009).
55. H. Sarlus, M. T. Heneka, Microglia in Alzheimer's disease. *J. Clin. Invest.* **127**, 3240–3249 (2017).
56. T. Takano, Role of microglia in autism: Recent advances. *Dev. Neurosci.* **37**, 195–202 (2015).
57. J. T. Morgan, G. Chana, C. A. Pardo, C. Achim, K. Semendeferi, J. Buckwalter, E. Courchesne, I. P. Everall, Microglial activation and increased microglial density observed in the dorsolateral prefrontal cortex in autism. *Biol. Psychiatry* **68**, 368–376 (2010).
58. D. L. Vargas, C. Nascimbene, C. Krishnan, A. W. Zimmerman, C. A. Pardo, Neuroglial activation and neuroinflammation in the brain of patients with autism. *Ann. Neurol.* **57**, 67–81 (2005).
59. M. J. Gandal, P. Zhang, E. Hadjimichael, R. L. Walker, C. Chen, S. Liu, H. Won, H. van Bakel, M. Varghese, Y. Wang, A. W. Shieh, J. Haney, S. Parhami, J. Belmont, M. Kim, P. Moran Losada, Z. Khan, J. Mleczko, Y. Xia, R. Dai, D. Wang, Y. T. Yang, M. Xu, K. Fish, P. R. Hof, J. Warrell, D. Fitzgerald, K. White, A. E. Jaffe; PsychENCODE Consortium, M. A. Peters, M. Gerstein, C. Liu, L. M. Iakoucheva, D. Pinto, D. H. Geschwind, Transcriptome-wide isoform-level dysregulation in ASD, schizophrenia, and bipolar disorder. *Science* **362**, eaat8127 (2018).

60. S. Gupta, S. E. Ellis, F. N. Ashar, A. Moes, J. S. Bader, J. Zhan, A. B. West, D. E. Arking, Transcriptome analysis reveals dysregulation of innate immune response genes and neuronal activity-dependent genes in autism. *Nat. Commun.* **5**, 5748 (2014).
61. A. S. Brown, E. S. Susser, In utero infection and adult schizophrenia. *Ment. Retard. Dev. Disabil. Res. Rev.* **8**, 51–57 (2002).
62. H. Onda, A. Lueck, P. W. Marks, H. B. Warren, D. J. Kwiatkowski, Tsc2(+/–) mice develop tumors in multiple sites that express gelsolin and are influenced by genetic background. *J. Clin. Invest.* **104**, 687–695 (1999).
63. A. S. Prabowo, J. J. Anink, M. Lammens, M. Nellist, A. M. W. van den Ouweland, H. Adle-Biassette, H. B. Sarnat, L. Flores-Sarnat, P. B. Crino, E. Aronica, Fetal brain lesions in tuberous sclerosis complex: TORC1 activation and inflammation. *Brain Pathol.* **23**, 45–59 (2013).
64. A. Deczkowska, O. Matcovitch-Natan, A. Tsitsou-Kampeli, S. Ben-Hamo, R. Dvir-Szternfeld, A. Spinrad, O. Singer, E. David, D. R. Winter, L. K. Smith, A. Kertser, K. Baruch, N. Rosenzweig, A. Terem, M. Prinz, S. Villeda, A. Citri, I. Amit, M. Schwartz, Mef2C restrains microglial inflammatory response and is lost in brain ageing in an IFN-I-dependent manner. *Nat. Commun.* **8**, 717 (2017).
65. K. Baruch, A. Deczkowska, E. David, J. M. Castellano, O. Miller, A. Kertser, T. Berkutzki, Z. Barnett-Itzhaki, D. Bezalel, T. Wyss-Coray, I. Amit, M. Schwartz, Aging. Aging-induced type I interferon response at the choroid plexus negatively affects brain function. *Science* **346**, 89–93 (2014).
66. A. Borsini, A. Cattaneo, C. Malpighi, S. Thuret, N. A. Harrison; MRC ImmunoPsychiatry Consortium, P. A. Zunszain, C. M. Pariante, Interferon-alpha reduces human hippocampal neurogenesis and increases apoptosis via activation of distinct STAT1-dependent mechanisms. *Int. J. Neuropsychopharmacol.* **21**, 187–200 (2018).
67. J. L. Silverman, M. Yang, C. Lord, J. N. Crawley, Behavioural phenotyping assays for mouse models of autism. *Nat. Rev. Neurosci.* **11**, 490–502 (2010).
68. M. F. López-Aranda, J. F. López-Téllez, I. Navarro-Lobato, M. Masmudi-Martín, A. Gutiérrez, Z. U. Khan, Role of layer 6 of V2 visual cortex in object-recognition memory. *Science* **325**, 87–89 (2009).
69. E. R. Fraley, Z. D. Burkett, N. F. Day, B. A. Schwartz, P. E. Phelps, S. A. White, Mice with Dab1 or Vldlr insufficiency exhibit abnormal neonatal vocalization patterns. *Sci. Rep.* **6**, 25807 (2016).
70. M. L. Scattoni, S. U. Gandhy, L. Ricceri, J. N. Crawley, Unusual repertoire of vocalizations in the BTBR T+tf/J mouse model of autism. *PLOS ONE* **3**, e3067 (2008).
71. N. N. Dagher, A. R. Najafi, K. M. N. Kayala, M. R. P. Elmore, T. E. White, R. Medeiros, B. L. West, K. N. Green, Colony-stimulating factor 1 receptor inhibition prevents microglial plaque association and improves cognition in 3xTg-AD mice. *J. Neuroinflammation* **12**, 139 (2015).
72. M. F. Lopez-Aranda, M. J. Acevedo, F. J. Carballo, A. Gutierrez, Z. U. Khan, Localization of the GoLoco motif carrier regulator of G-protein signalling 12 and 14 proteins in monkey and rat brain. *Eur. J. Neurosci.* **23**, 2971–2982 (2006).
73. M. C. Oldham, P. Langfelder, S. Horvath, Network methods for describing sample relationships in genomic datasets: Application to Huntington's disease. *BMC Syst. Biol.* **6**, 63 (2012).
74. C. W. Law, Y. Chen, W. Shi, G. K. Smyth, voom: Precision weights unlock linear model analysis tools for RNA-seq read counts. *Genome Biol.* **15**, R29 (2014).
75. Y. Zhang, S. A. Sloan, L. E. Clarke, C. Caneda, C. A. Plaza, P. D. Blumenthal, H. Vogel, G. K. Steinberg, M. S. B. Edwards, G. Li, J. A. Duncan III, S. H. Cheshier, L. M. Shuer, E. F. Chang, G. A. Grant, M. G. H. Gephart, B. A. Barres, Purification and characterization of progenitor and mature human astrocytes reveals transcriptional and functional differences with mouse. *Neuron* **89**, 37–53 (2016).
76. K. Strimmer, fdrtool: A versatile R package for estimating local and tail area-based false discovery rates. *Bioinformatics* **24**, 1461–1462 (2008).

Acknowledgments: We thank C. Thadani, E. Lugo, O. Lu, and K. Dingle for contributions to the development, maintenance, and treatment of the experimental mice. Thanks to A. F. de Sousa for help with the statistical analyses, as well as to the members of the Silva laboratory for discussions that contributed to experiments and analyses described here. Special thanks to Plexxikon Inc. for providing both PLX and control chow. **Funding:** This work was supported by the Human Frontier Science Program (reference no. LT000822/2011-L), Children's Tumor Foundation (grant no. 2014-01-014), Takeda Pharmaceutical Company Limited, and NIH R01 MH084315 to A.J.S. **Author contributions:** Conceptualization: A.J.S. and M.F.L.-A. Methodology: A.J.S. and M.F.L.-A. Validation: T.K.S. Formal analyses: M.F.L.-A., G.M.B., E.R.F., M.G., I.C., and A.R. Investigation: M.F.L.-A., G.M.B., E.R.F., M.P., I.H., S.T., R.M., and K.B. Resources: M.Z., D.H.G., G.C., S.A.W., and Plexxikon Inc. Writing—Original draft: M.F.L.-A. and A.J.S. Writing—Review and editing: A.J.S. and M.F.L.-A. Visualization: A.J.S. and M.F.L.-A. Supervision: A.J.S. Funding acquisition: A.J.S and M.F.L.-A. **Competing interests:** The authors declare that they have no competing interests. **Data and materials availability:** PLX5622 was obtained under a material transfer agreement with Plexxikon. All data needed to evaluate the conclusions in the paper are present in the paper and/or the Supplementary Materials.

Submitted 11 October 2020
Accepted 27 July 2021
Published 17 September 2021
10.1126/sciadv.abf2073

Citation: M. F. López-Aranda, I. Chattopadhyay, G. M. Boxx, E. R. Fraley, T. K. Silva, M. Zhou, M. Phan, I. Herrera, S. Taloma, R. Mandanas, K. Bach, M. Gandal, D. H. Geschwind, G. Cheng, A. Rzhetsky, S. A. White, A. J. Silva, Postnatal immune activation causes social deficits in a mouse model of tuberous sclerosis: Role of microglia and clinical implications. *Sci. Adv.* **7**, eabf2073 (2021).